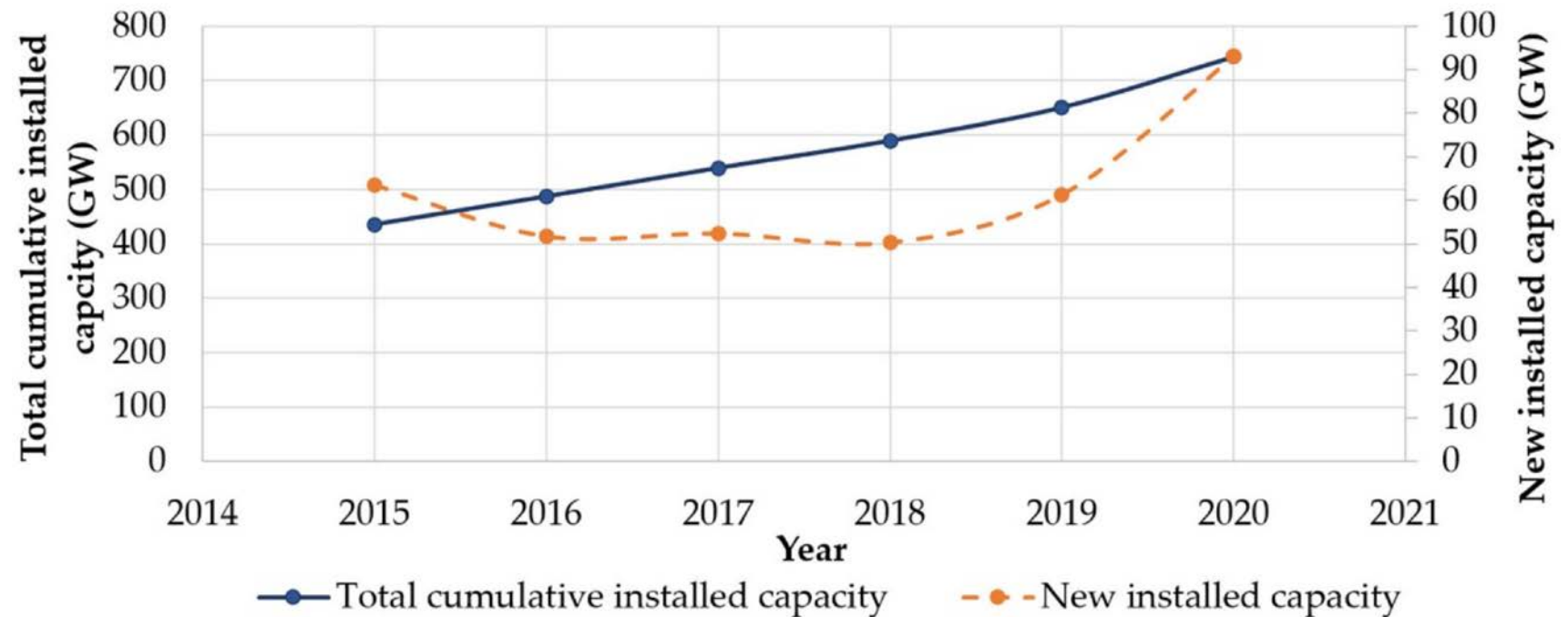


Wind Turbine Blade Damage due to hail impact and lighting strike

Professor V. Kostopoulos

Wind Turbine renewable energy sources (RES)



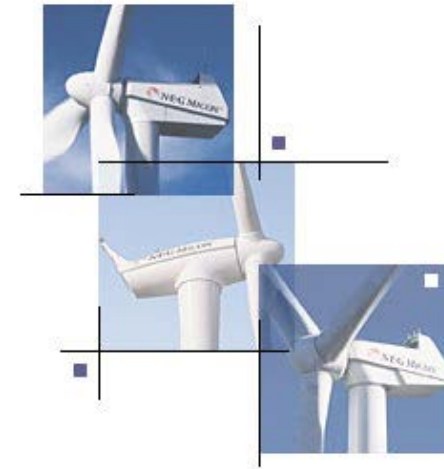
Evolution since 2015 in worldwide installed wind park generating capacity

Wind Turbine renewable energy sources (RES)

- A total of 744 GW in wind park generating capacity had been installed worldwide as of the end of 2020, of which 93 GW were added during 2020 alone.
- 308.7 GW of new wind park generating capacity has been installed worldwide since 2015, corresponding to a 70% increase in total capacity.
- The annual share of global electricity production attributable to wind energy was estimated at 6% in 2020, or roughly 1600 TWh, and is expected to rise to 30% by 2050.

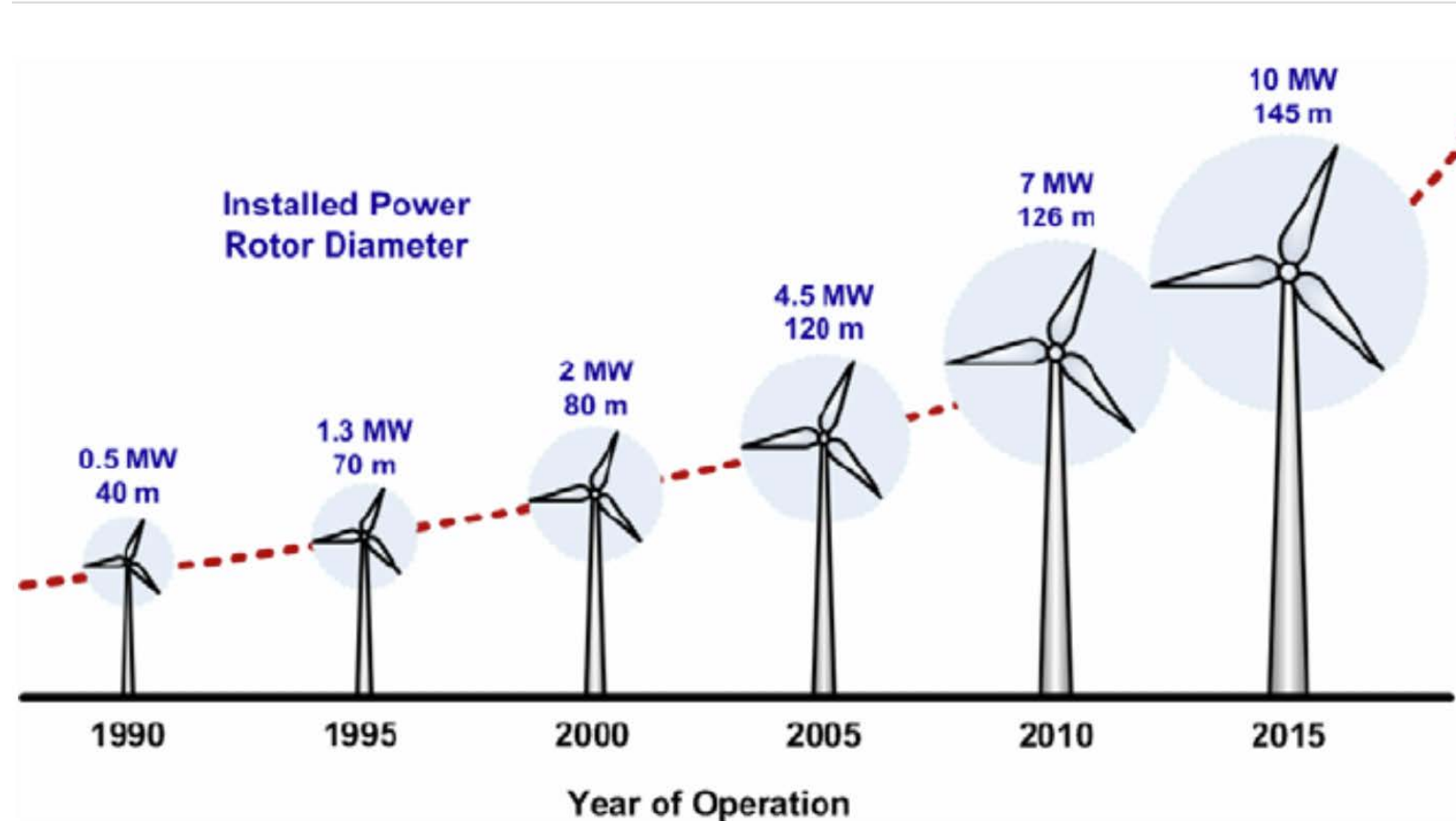
Damage to wind turbine blades

- **Lightning strike**
- **Hail Impact**
- **Mechanical Fatigue**
- **Leading edge erosion**
- **Ice accumulation on the blade surface**

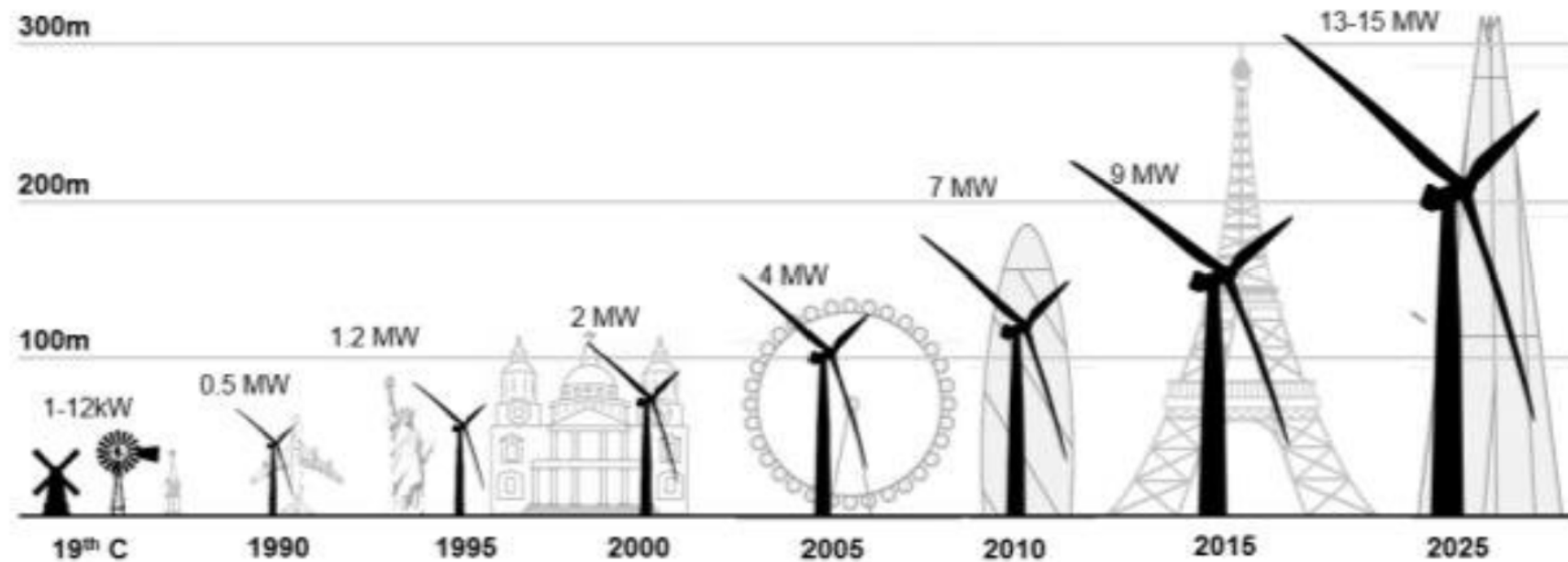


Size evolution of Wind Turbines

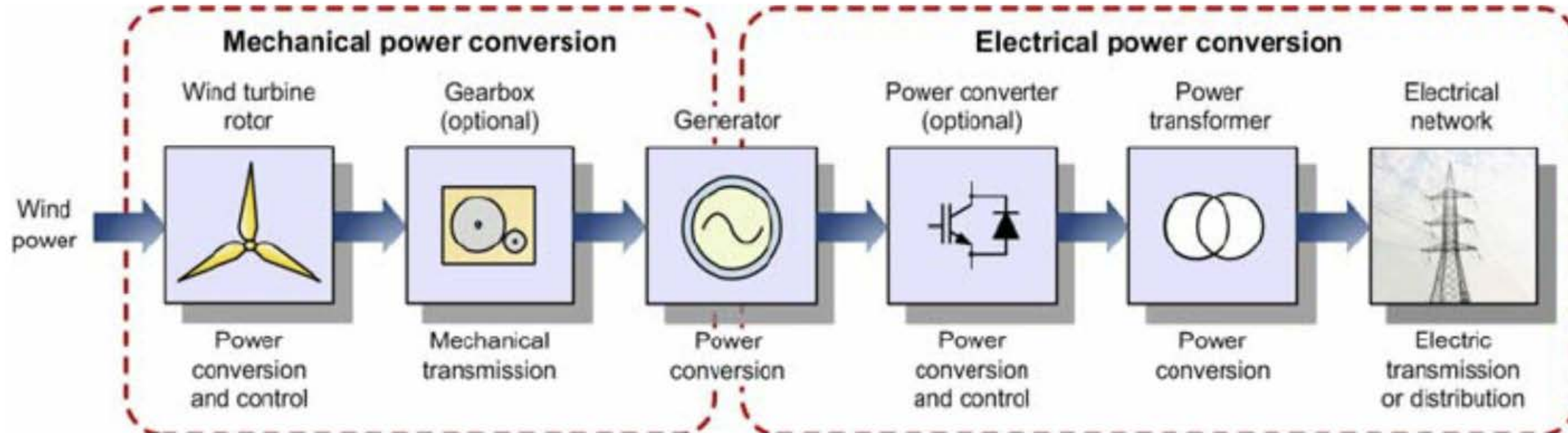
Nowadays, the size of wind turbines has increased dramatically



Size evolution of wind turbines over time

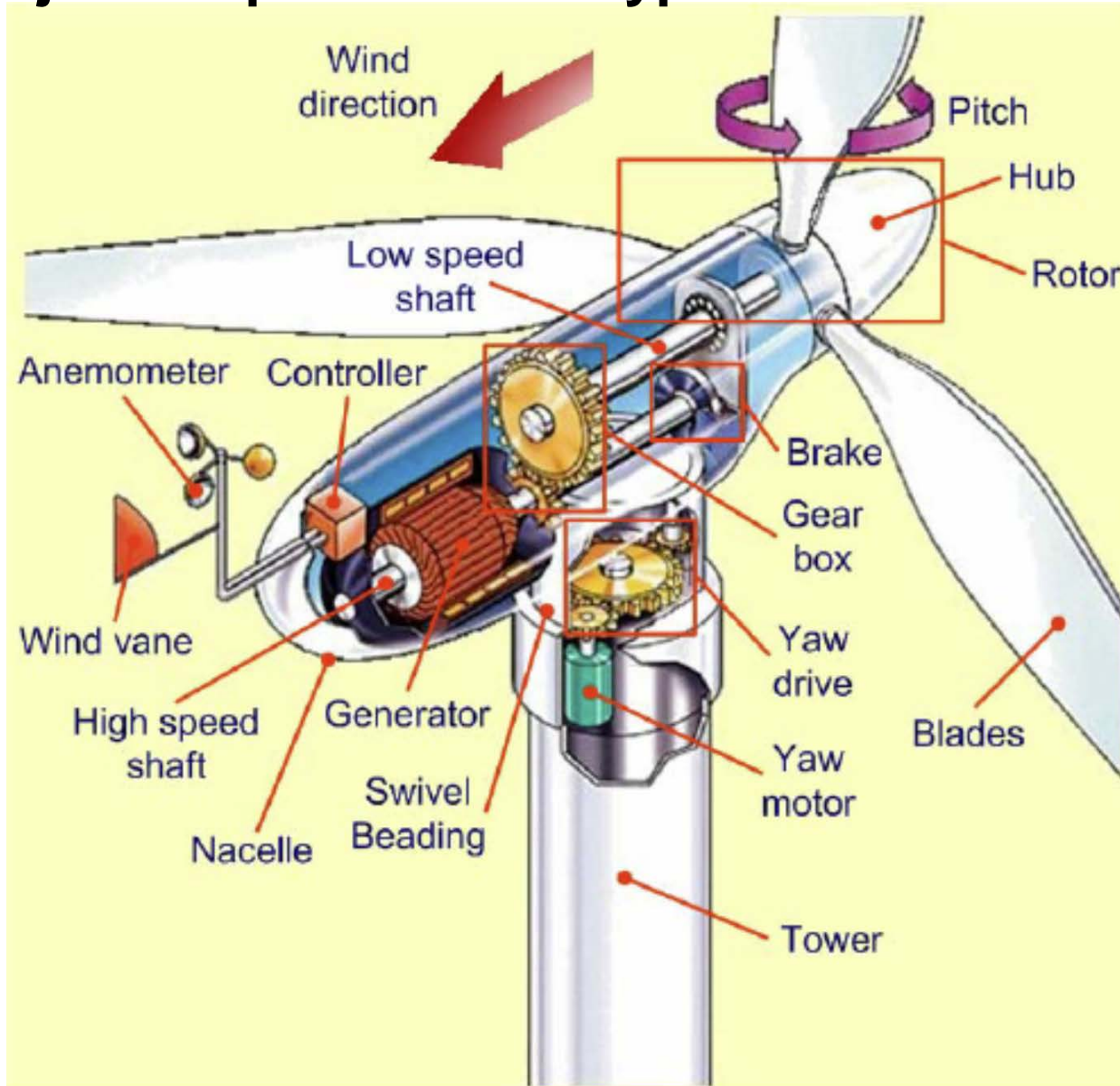


General description of a wind turbine system



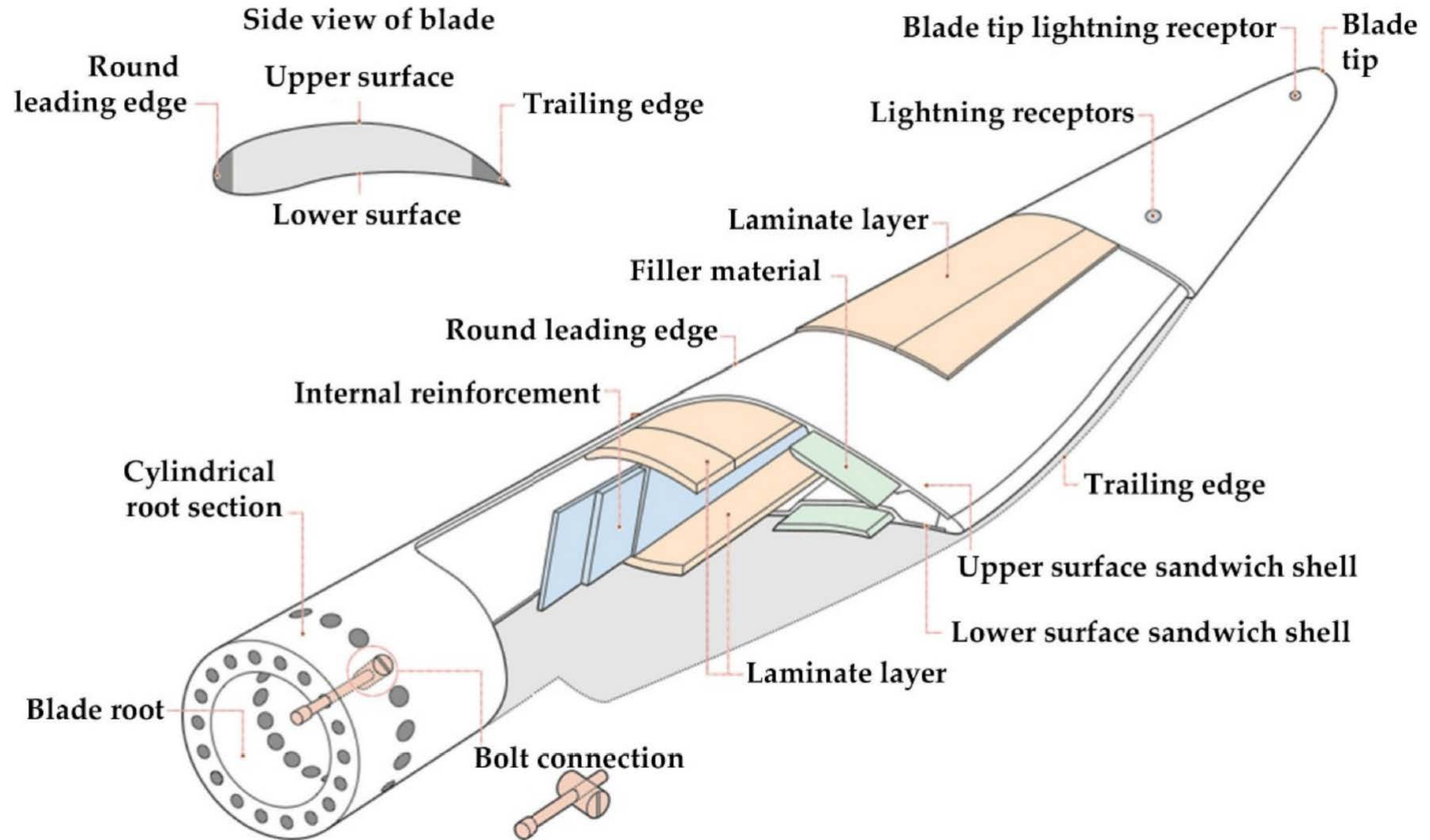
The appropriate voltage level is related to the generated power level. A modern wind turbine is often equipped with a transformer stepping up the generator terminal voltage, usually a voltage below 1 kV (E.g. 575 or 690 V), to a medium voltage around 20-30 kV, for the local electrical connection within a wind farm (distribution level).

Major components of a typical horizontal axis, three-bladed, upwind wind turbine

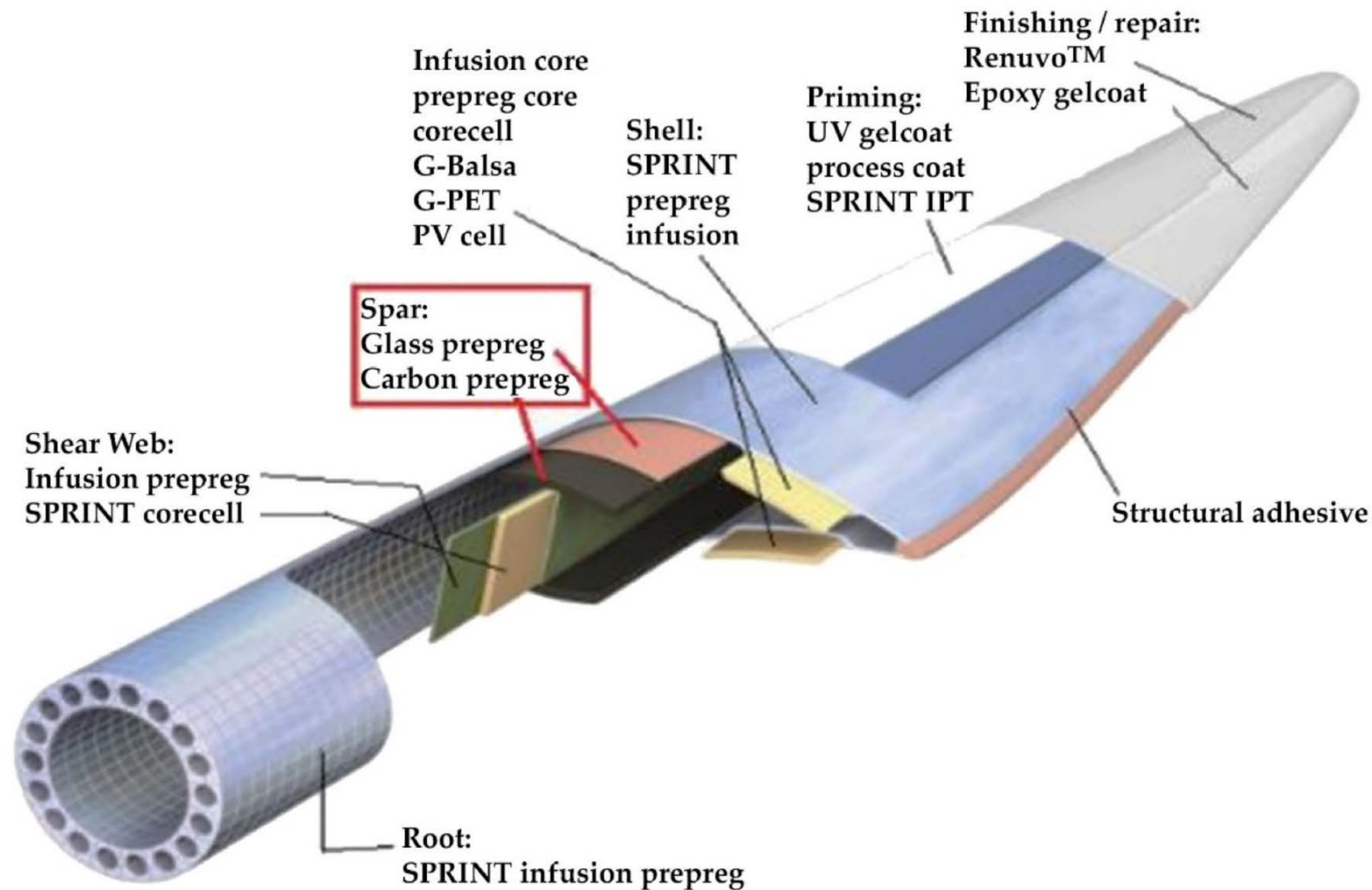


Major components of a typical horizontal axis, three-bladed, upwind wind turbine

Typical wind turbine blade

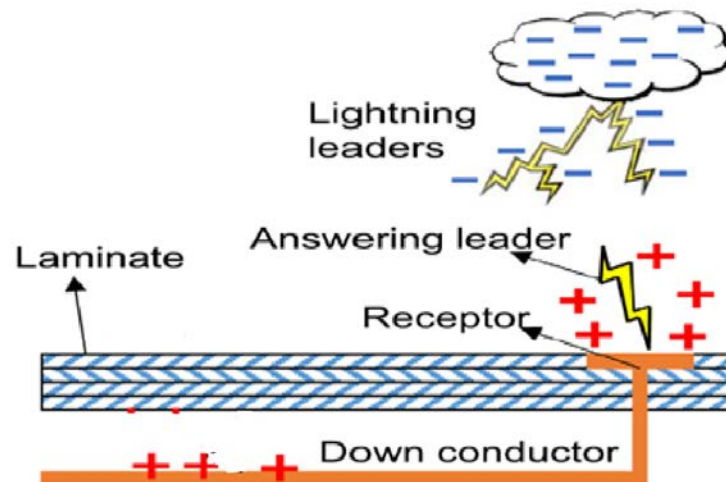


Typical wind turbine blade structure

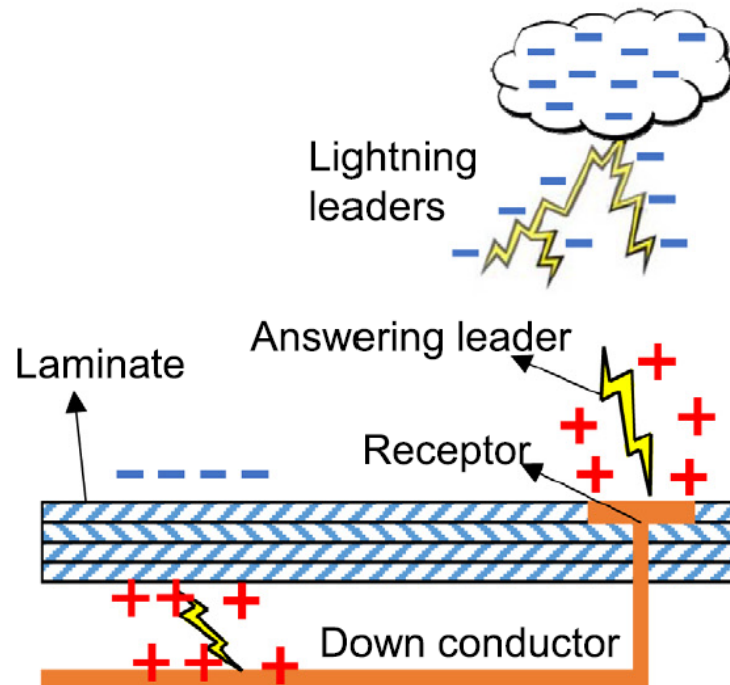


Lighting Strike of Wind Turbine Blades

- Lightning discharge is essentially a dielectric breakdown of the air, which is initiated by a large electric field established between the cloud and the earth or between two clouds. For a typical negative-polarity downward-initiated cloud-to-ground lightning discharge, the lightning leaders are initiated from the lower part of the cumulonimbus cloud (with negative charges) and propagate through the air approaching the ground.
- When the lightning leader tip arrives within a certain distance (striking distance) of a grounded structure, the answering leaders emitted from the grounded structures due to the lightning electric field attempt to capture the approaching lightning leaders. Once they are connected, the first lightning return stroke occurs. Thus, the lightning attachment point on the structure is determined before any lightning current is conducted.
- Structures that emit answering leaders are commonly conductive such as metallic conductors. However, non-conductive structures (e.g., GFRP composites) are also able to emit answering leaders if conductive contamination is present.

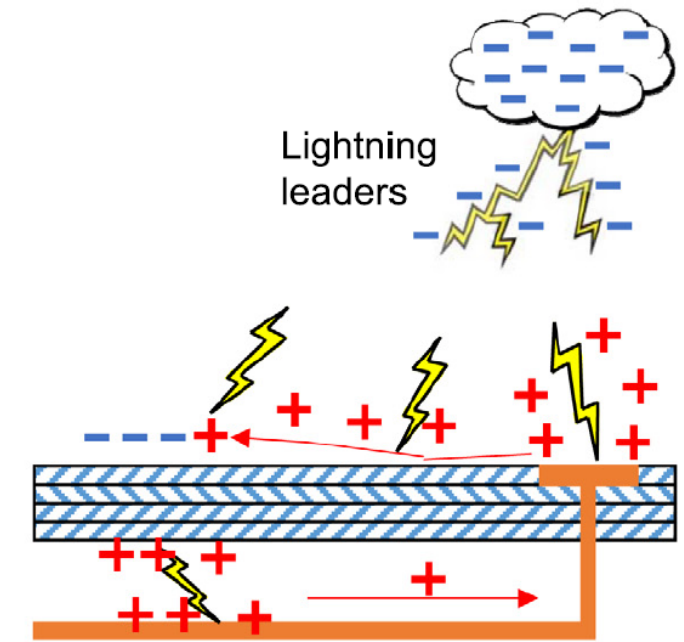
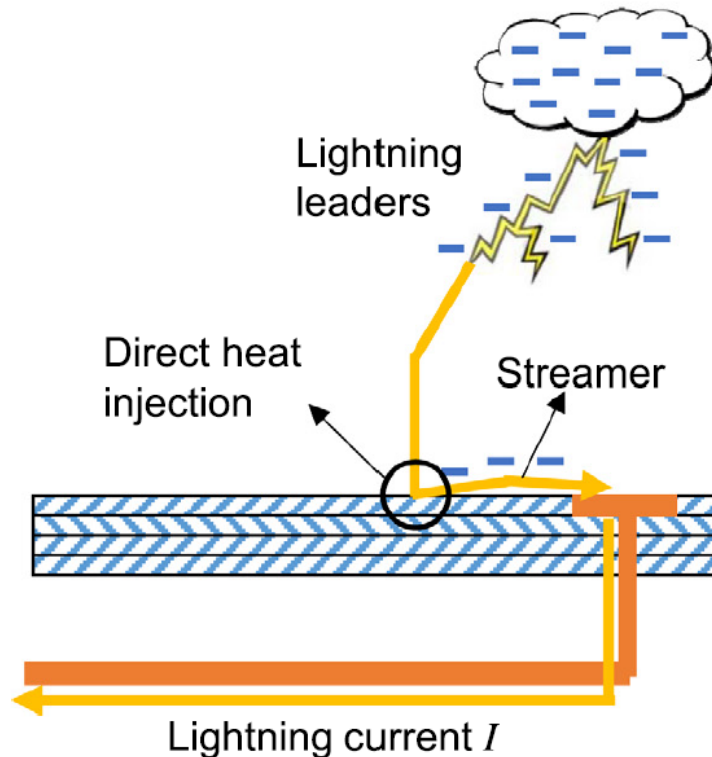


- GFRP composite wind turbine blades are designed with lightning strike protection (LSP) that includes receptors attached to the blades and connected to the down conductors installed in the blade interior. The receptors are designed to emit answering leaders, so the lightning current can be safely conducted through the down conductor to the ground.
- However, experience has shown that blades equipped with receptors and down conductors system are still subjected to lightning strike damage. This is because the answering leaders are not only emitted from receptors, but also are emitted from the internal down conductor due to molecule ionization under the lightning electric field. The resulting positive charges are deposited on the interior surface of the blade and induce negative charges on the exterior surface.

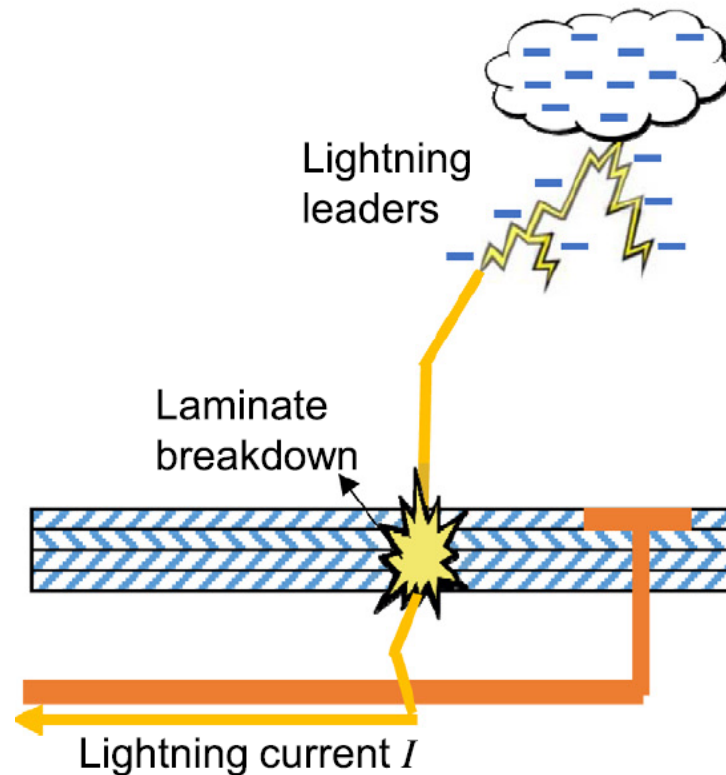


- In addition, the contaminated areas (e.g., moisture, dirt, salt, bugs, etc.) on the insulated (i.e., GFRP composite) blade surface under a sufficient electric field are also capable of generating answering leaders. In most cases, the answering leaders emitted from the receptors reach the lightning leader tip first. However, because of the presence of the negative charges on the exterior surface, the positive charges on the receptor search for and neutralize those negative charges. In this case, the positive charges along the searching path (insulated area) can also emit answering leaders.

If one of them connects with the approaching lightning leader, a surface flashover (streamer) occurs from the lightning attachment point to the closest receptor.



Then the lightning attachment at the insulated surface comes as a direct heat injection into the surface leading to a significant temperature increase at the surface and resulting in appreciable thermal damage. If the electric field at the attachment point is sufficient, a breakdown of the GFRP composite occurs and severe damage develops.





Blade damages due to lightning.

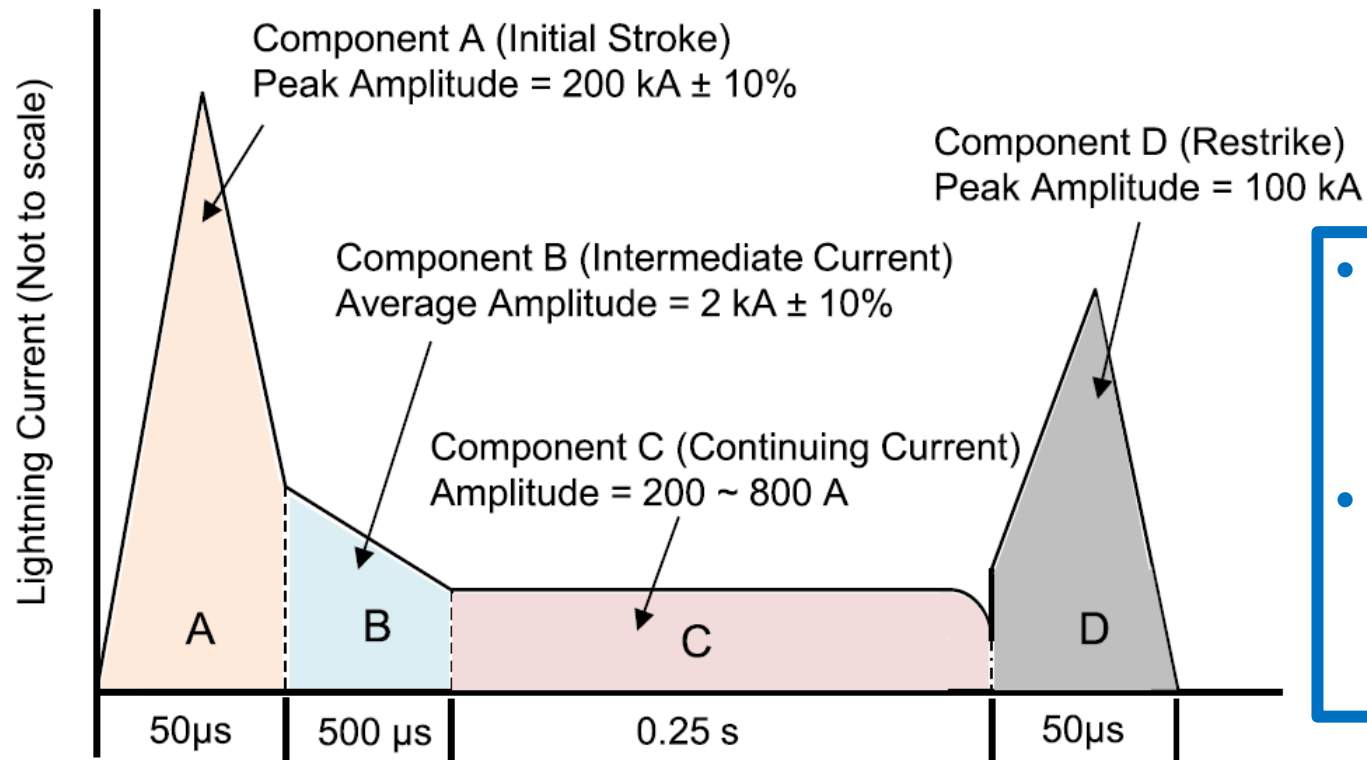


Lightning discharge to rotating blade.



Lightning current waveform and associated heat flux

- Lightning thermal damage depends on the severity, duration, and waveform characteristics of the lightning current.
- Typically, a lightning strike consists of four strokes: initial stroke, intermediate stroke, continuing stroke, and return stroke.



- Component C is the primary lightning current source that contributes to the majority of lightning strike thermal damage,
- Component A is responsible for the rapid expansion of the lightning plasma channel and, thus, controls the extent of the thermal damage area.

Fig. 2. Lightning current MIL-STD-464.

Lightning current flows in a narrow cylindrical plasma channel whose size depends on the current waveform, pressure, density, etc.

One of the first models describing dependence of the channel radius on the current was presented by Braginskii

$$R(t) = \alpha \rho_0^{-1/6} [I(t)]^{1/3} t^{1/2}$$

where $R(t)$ is the channel radius (in meters) that expands in time, α is a constant; $\alpha = 0,294$, ρ_0 is the air density at atmosphere pressure, $\rho_0 = 1,29 \text{ kg/m}^3$, $I(t)$ is an instant current in amperes (the current is presumed to increase linearly with time) and t is time in seconds.

The experimental and numerical results indicate that continuous expansion of the lightning channel occurs during the decaying part of component A, while expression for $R(t)$ predicts a reduction in the channel radius as the electric current decays. To overcome this problem, it is suggested to use I_{peak} instead of $I(t)$.

Lightning-current-induced heat flux at the surface of the structure is confined to the lightning arc channel.

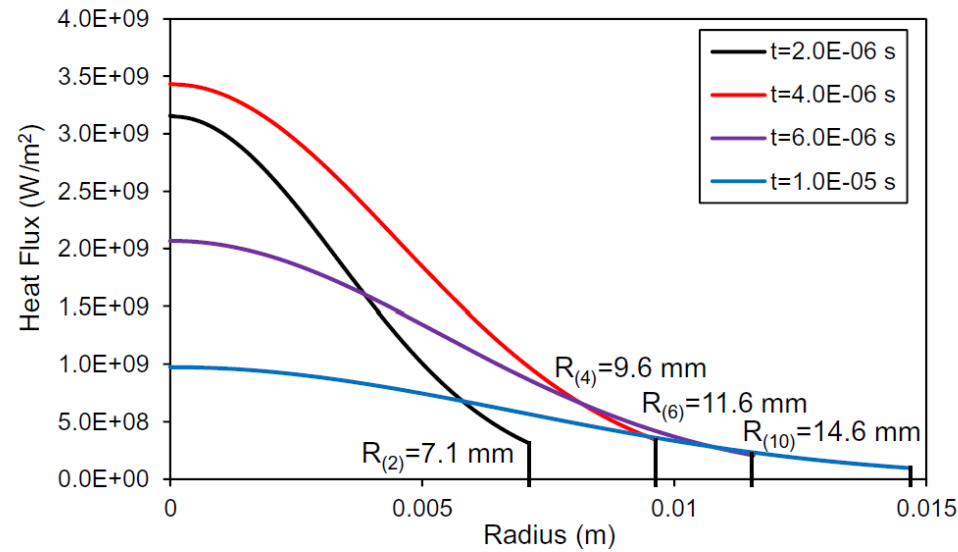


Fig. 7. Heat flux distribution over the circular area of the arc channel at different moments of time during component A.

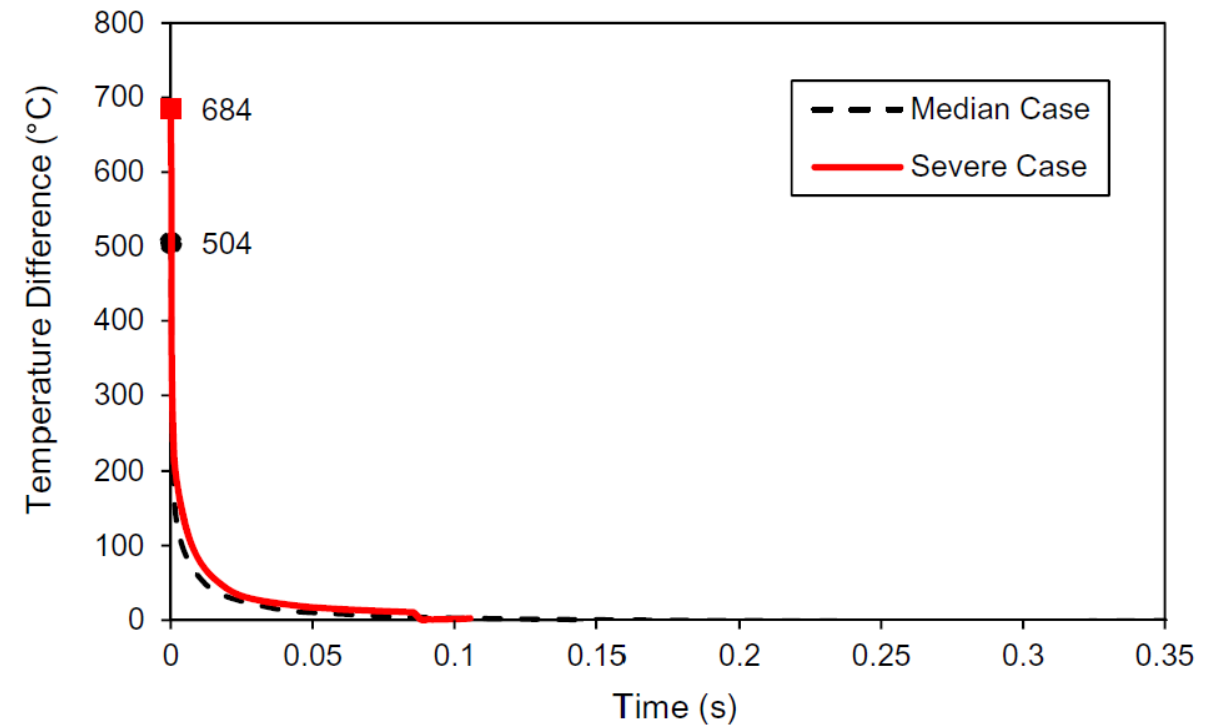


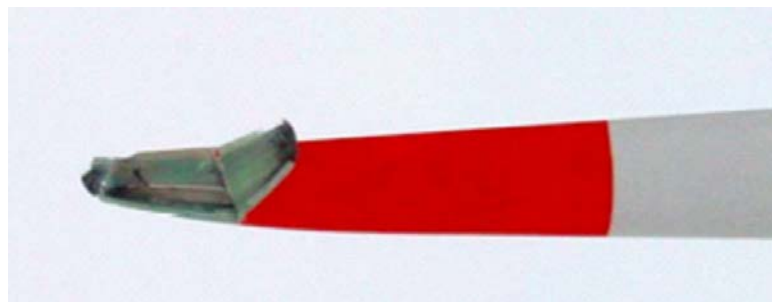
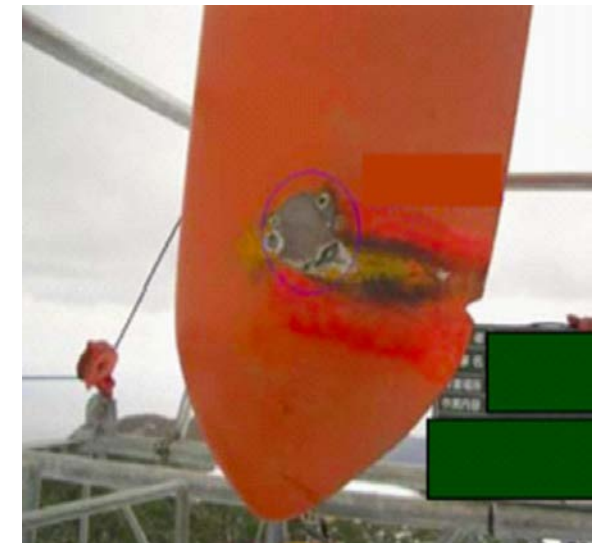
Fig. 10. Temperature difference vs. time at $r = 0$ for fully coupled (components A and C) and weakly coupled (component C) analyses.



(c) Damaged area



Ruptured blade due to gradual cracking after Lighting strike

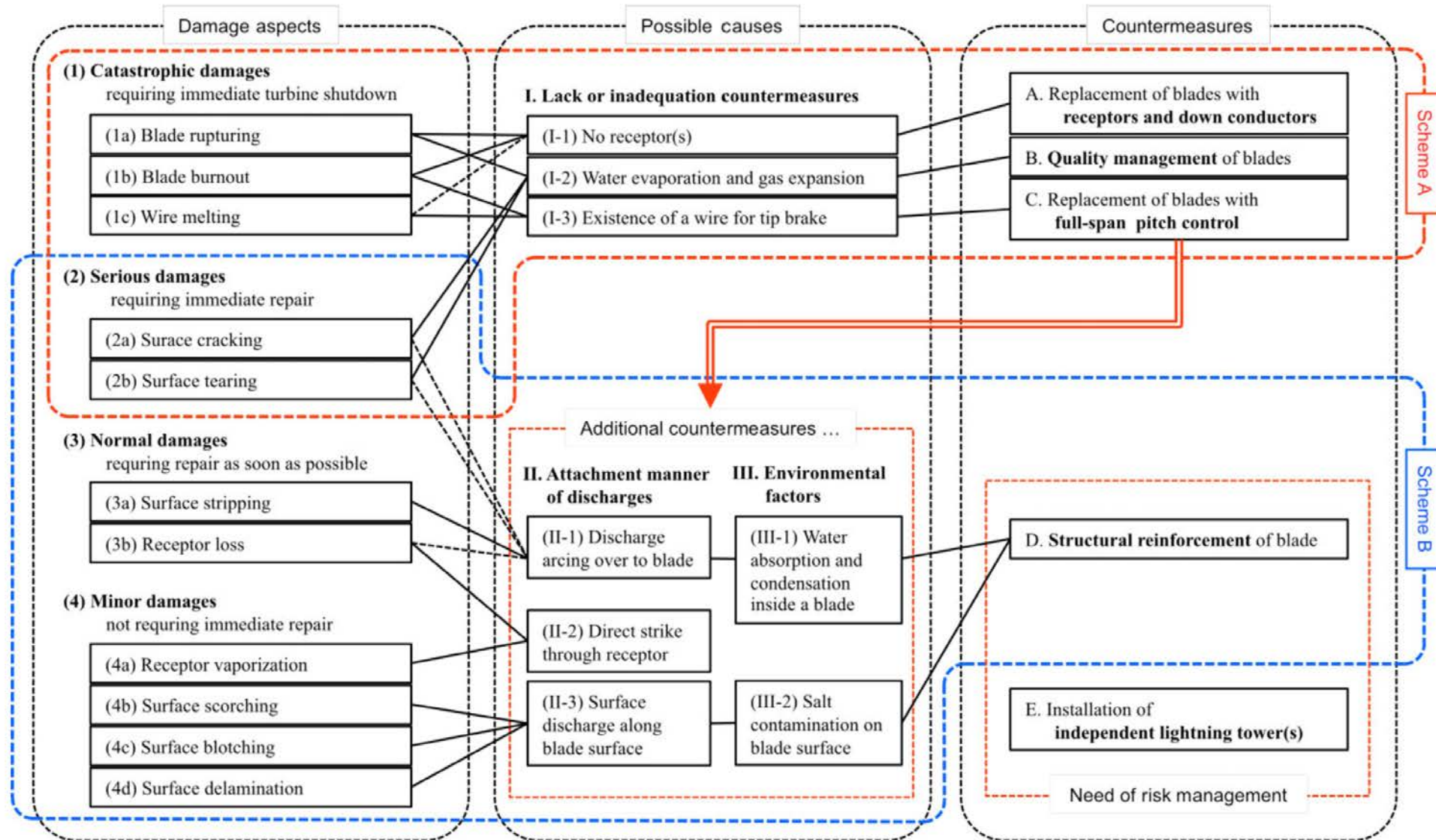


Proposed classification of blade damage

Levels (and subcategories) of damages

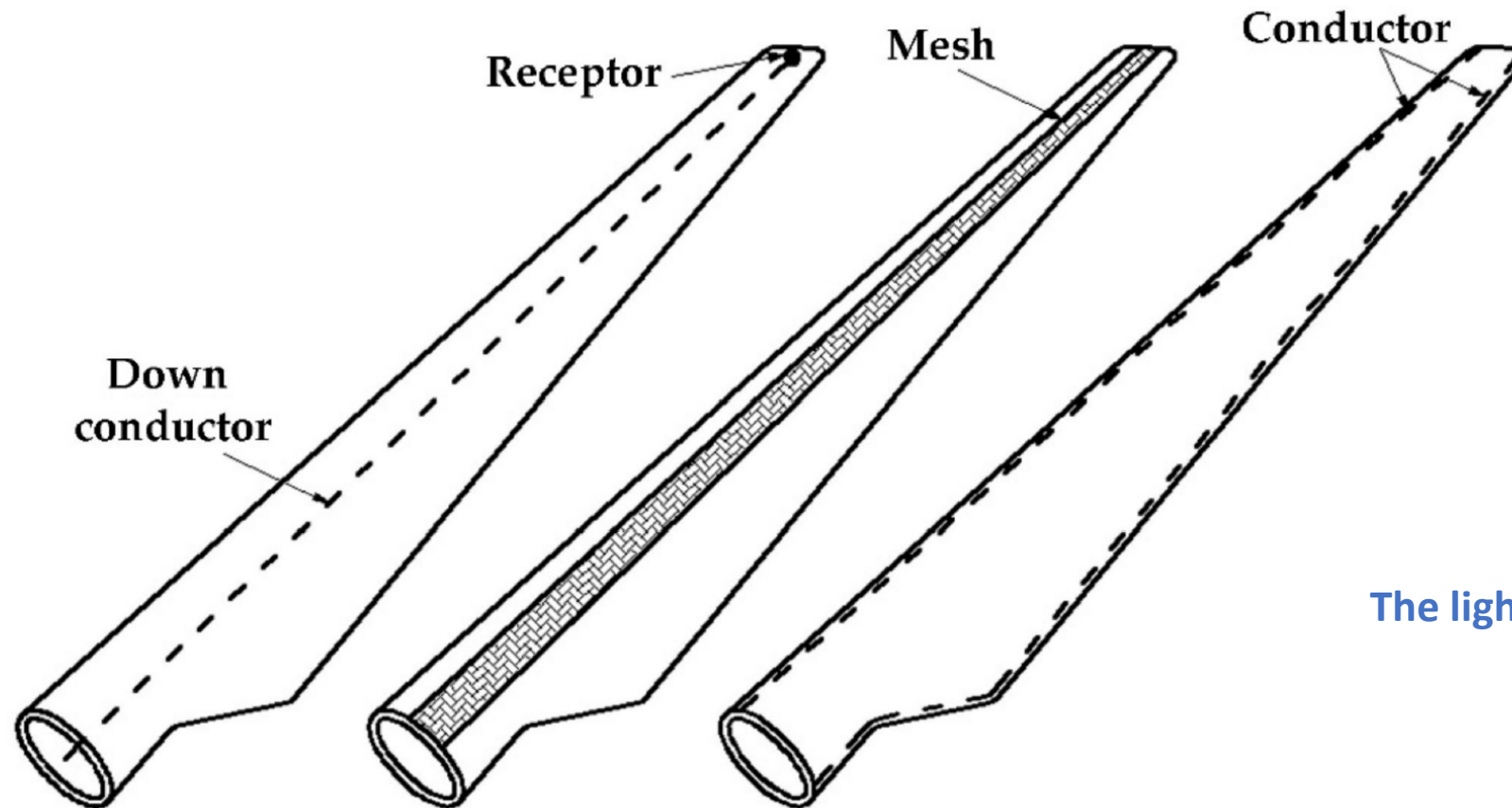
1. Catastrophic damage requiring immediate turbine shutdown
 - (a) Blade rupturing
 - (b) Blade burnout
 - (c) Wire melting
 2. Serious damage requiring immediate repair
 - (a) Surface cracking
 - (b) Surface tearing
 3. Normal damage requiring repair as soon as possible
 - (a) Surface stripping
 - (b) Receptor loss
 4. Minor damage not requiring immediate repair
 - (a) Receptor vaporization
 - (b) Surface scorching
 - (c) Surface blotching
 - (d) Surface delamination
-

- More than 60% of the total damage occurred within the last meter of the blade, and 90% of all damage was located within the last 4 m. The remaining 10% of damage was found mainly from 5 m to 10 m from the blade tip.
- The most common type of lightning damage was delamination (72% of total blade damage), followed by debonding of the shells (24%). Shell and tip detachment each occurred in 2% of the reported cases.
- Wind turbines suffering damage to more than one blade are uncommon (3 % in two blades and 1 % in three blades).



Schematic diagram of relationship between damage aspects and their countermeasures

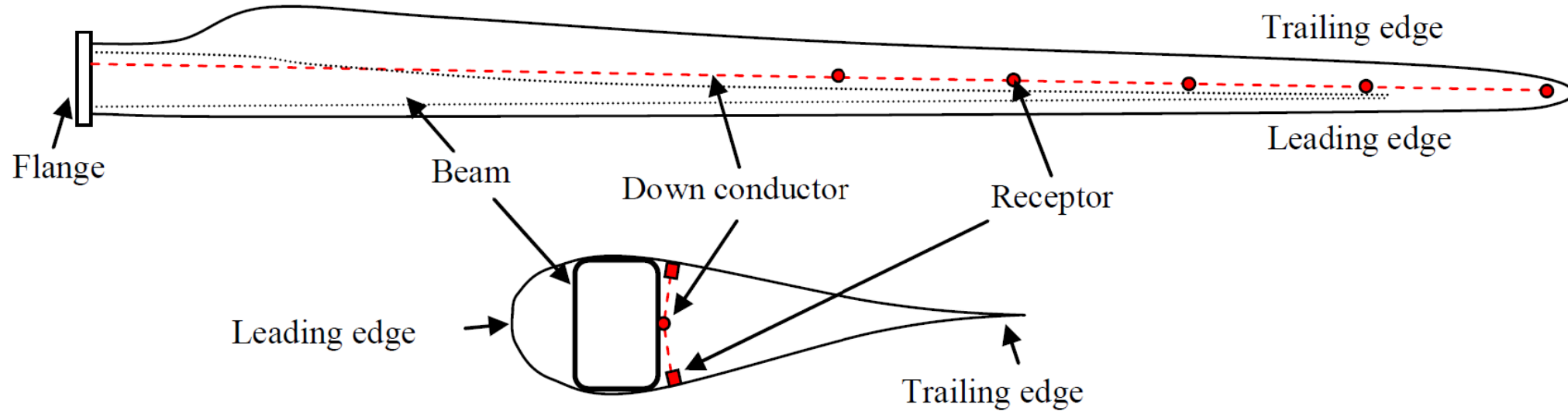
Lighting Strike Protection of Wind Turbine Blades



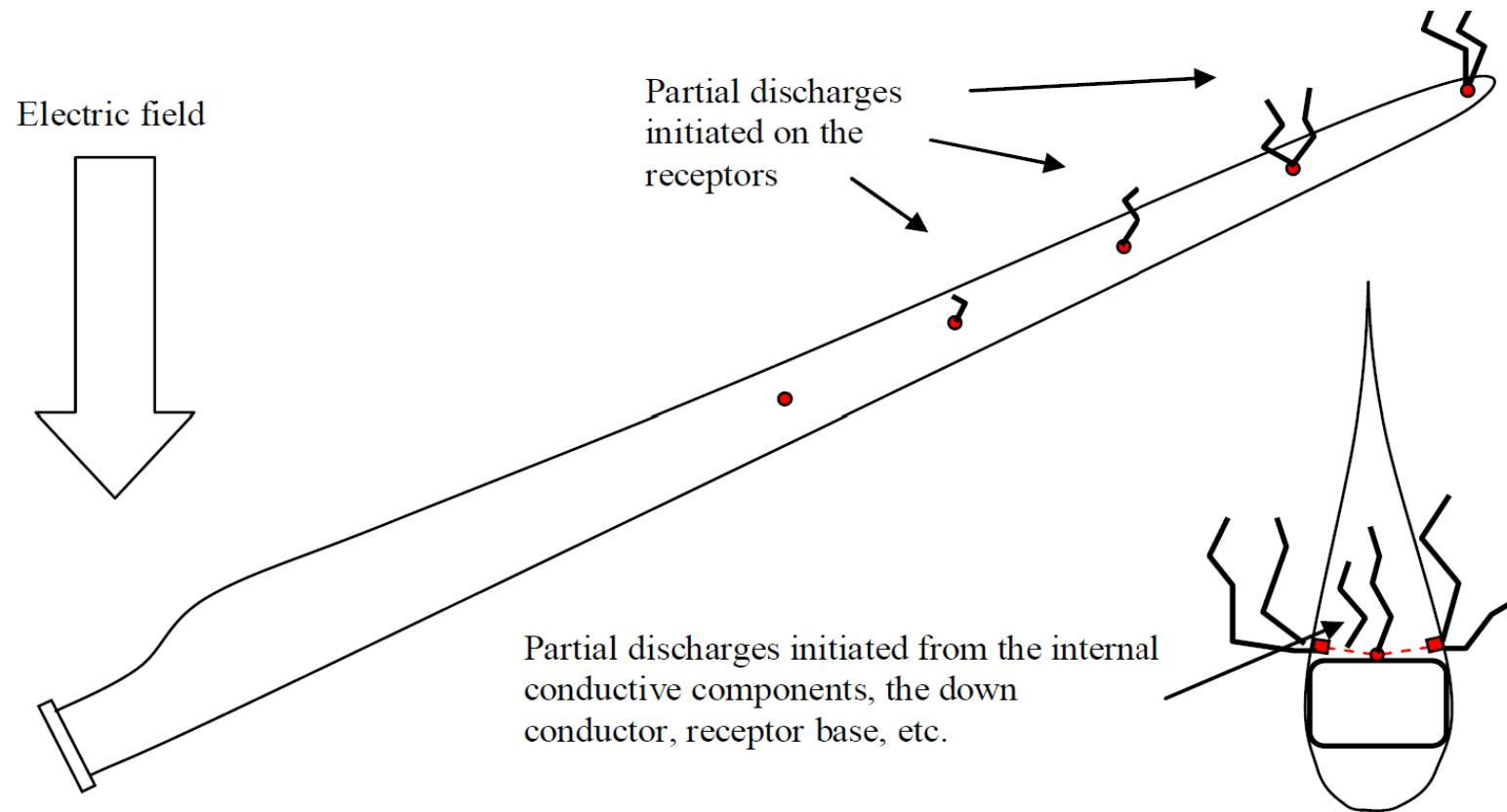
The lightning tower approach

- air termination systems on the blade surfaces
- high resistive tapes and diverters
- down conductors placed inside the blade
- conducting materials for the blade surface

Lighting Strike Protection of Wind Turbine Blades

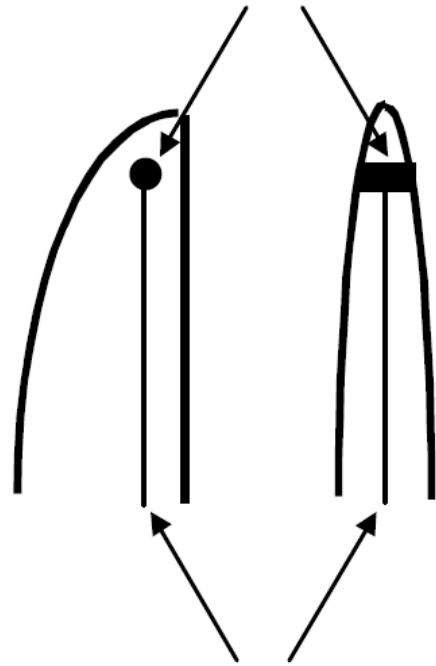


discrete receptors connected to an internal down conductor



Discharges on new and clean blade, mainly from metallic components.

Lightning receptor placed flush with blade surface and connected to internal conductor

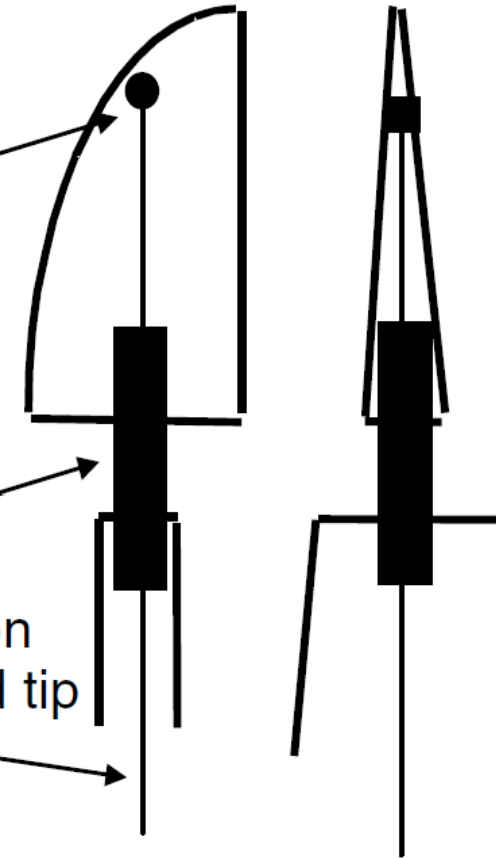


Internal conductor connected to earth

Lightning receptor

Carbon fibre shaft

Combined lightning protection system down conductor and tip brake control cable



Internal lightning protection system for pitch- and stall-regulated blades

Leading edge erosion of wind turbine blades



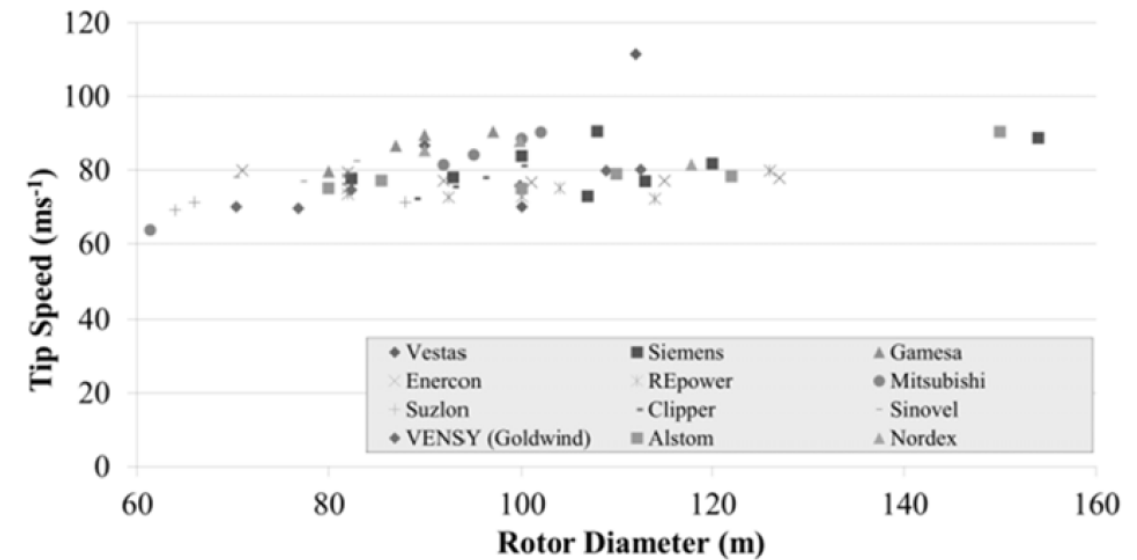
As with all forms of environmental exposure, leading edge erosion is heavily site-dependent.

In warm and arid climates, sand and dust may be a common type of airborne particulate and therefore may pose leading edge erosion problems, whereas in wetter, greener habitats, the problem may be non-existent ...

Leading edge erosion of wind turbine blades



leading edge erosion.

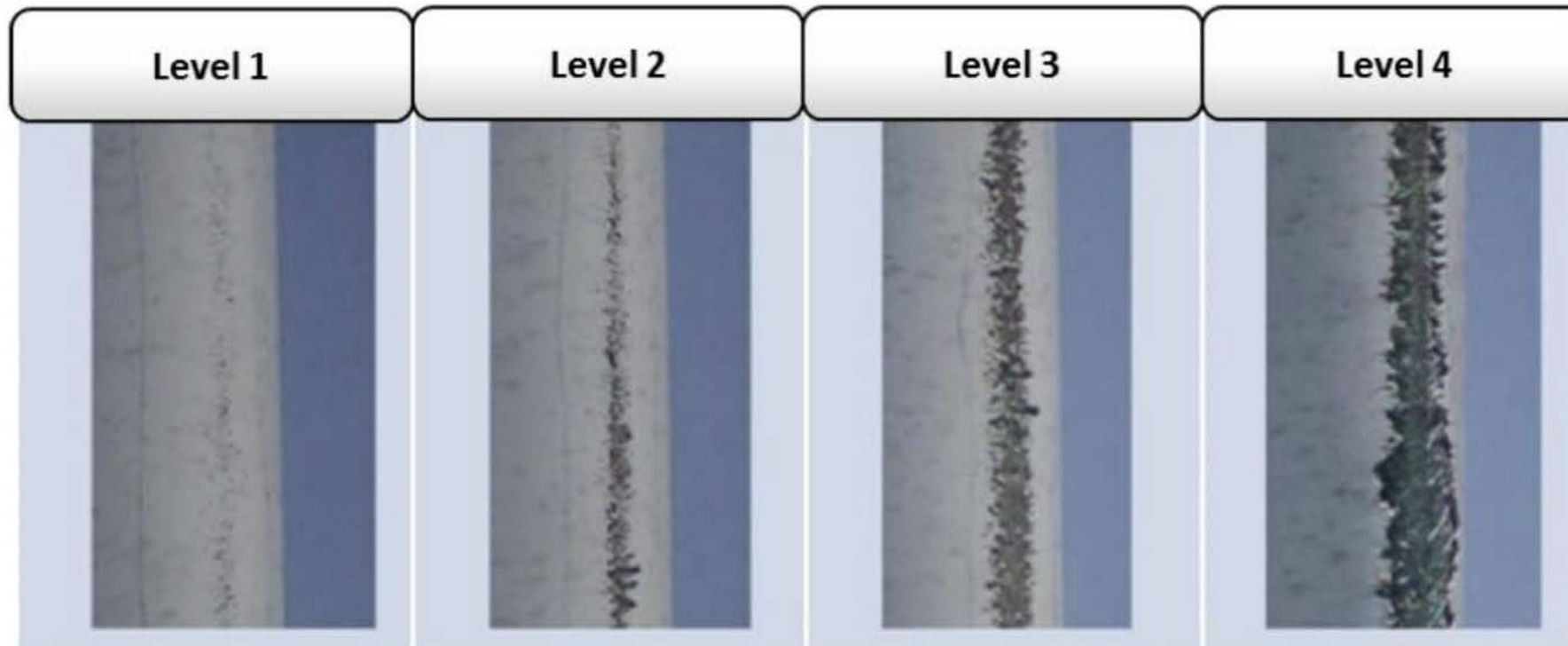


- Matrix material and composites are sensitive to environmental factors such as heat, moisture, salinity and UV radiation as well rain droplets, hailstone, sea-spray, dust and sand
- The first negative impact of the exposure of the composite blade to this is a gradual increase in the blade's surface roughness, which negatively affects the blade's aerodynamic performance by increasing its friction drag, and aerodynamic loss on the scale of 0.45–0.50%

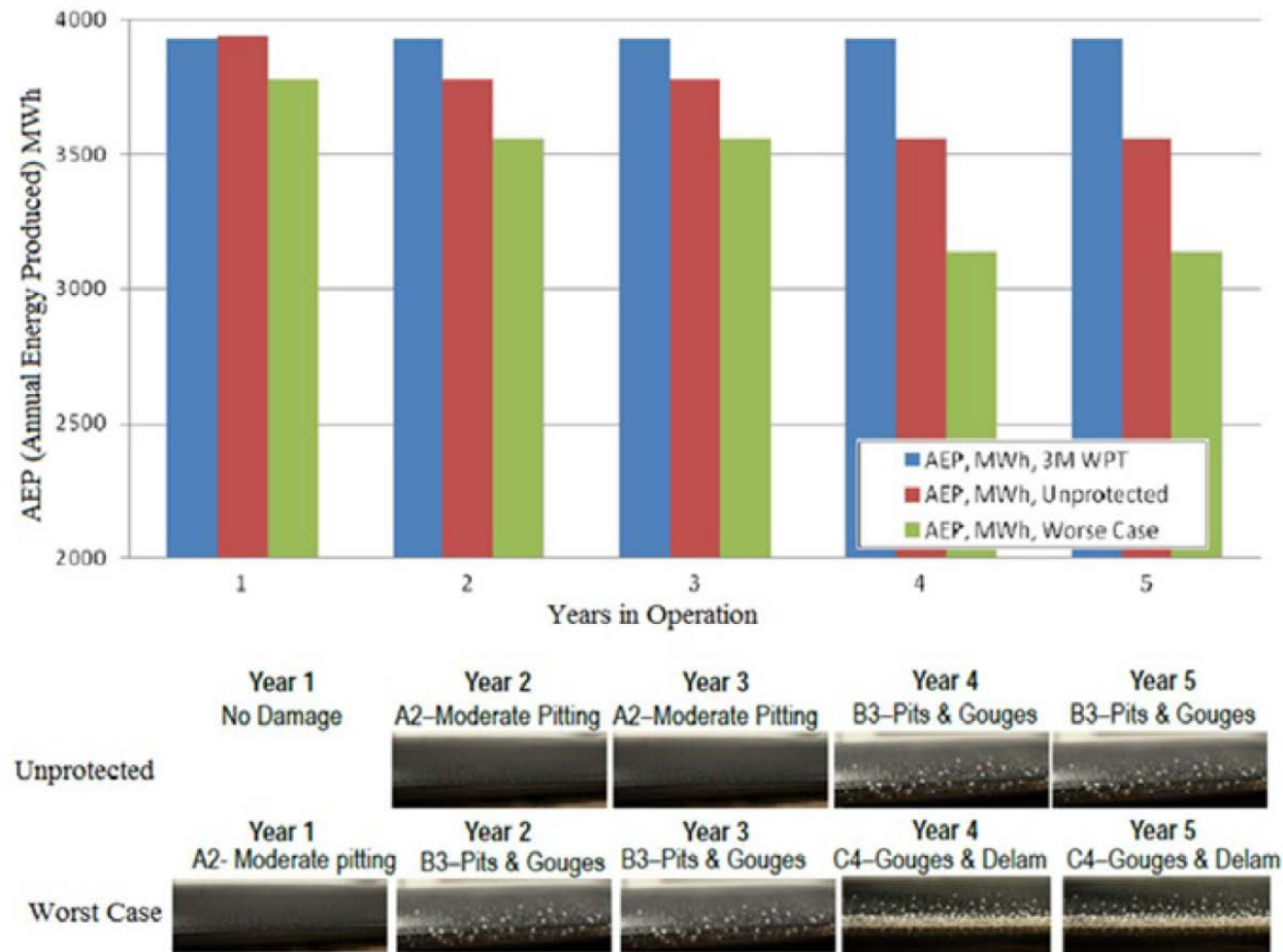
To address these problems effective protective surface coatings are used

The main purposes of protective coating systems are:

- (1) To act as a barrier from environmental factors such as UV and moisture which can affect the material properties of the composite structure
- (2) to protect the composite substrate from foreign body impact, whether that is during manufacture and handling, installation and maintenance **or from rain, hailstone and other forms of impact during operation.**



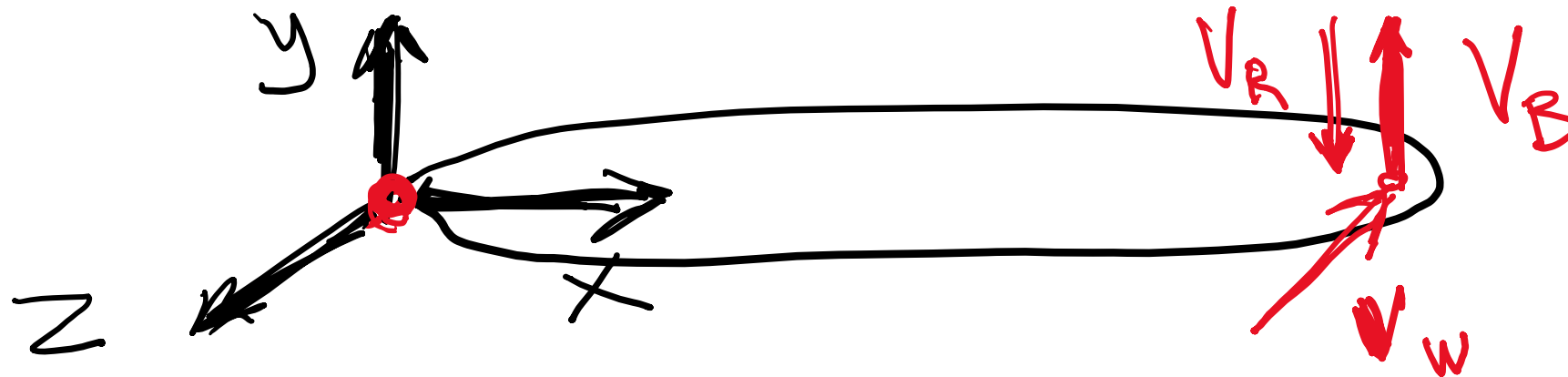
Leading Edge Erosion produces reduction in aerodynamic and power production efficiency



Calculated effects of varying levels of leading edge erosion on the annual energy production of a 1.5 MW wind turbine.

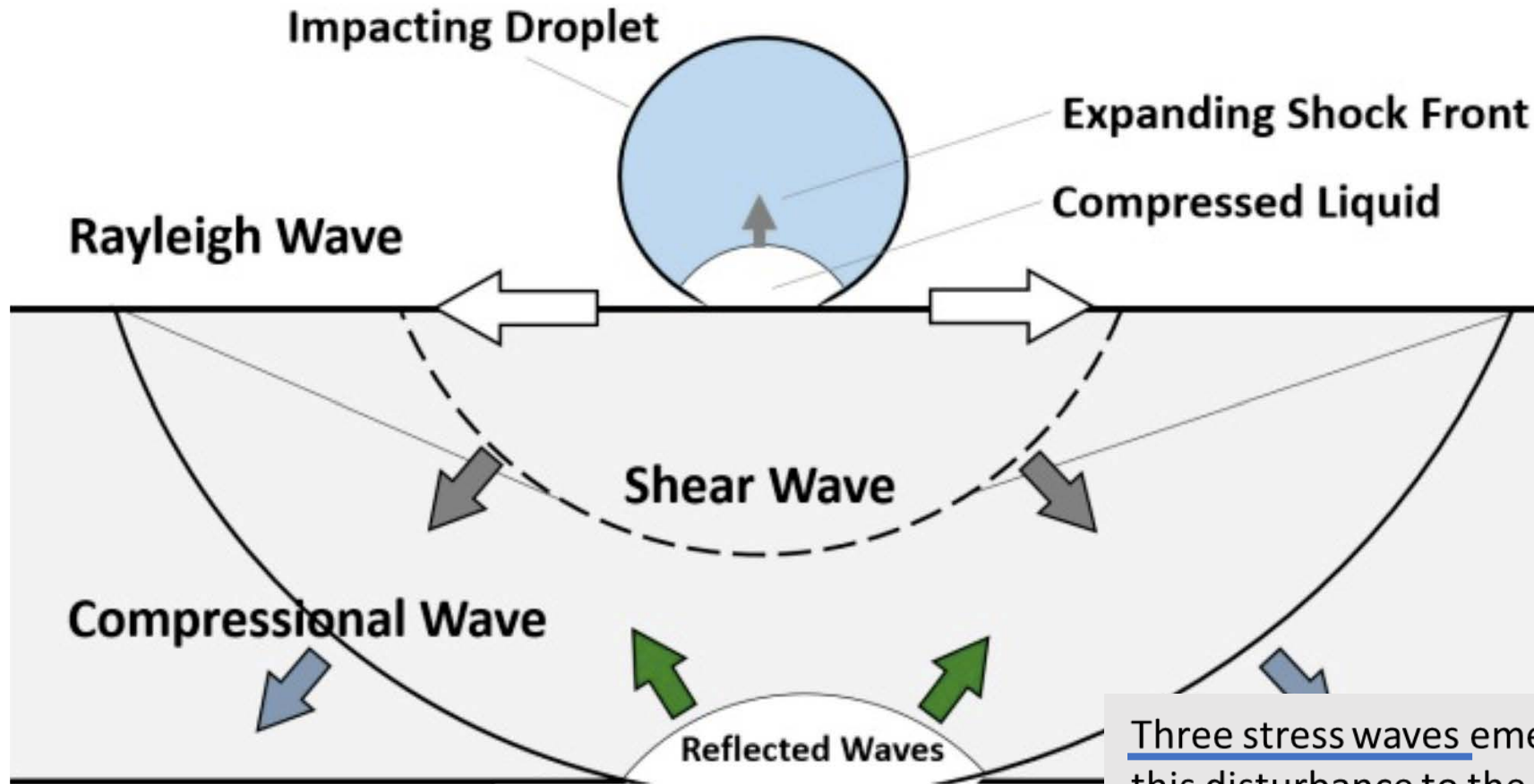
A rough estimation of the forces acting on a blade coating from raindrops is given bellow:

- Typical raindrop diameters are commonly cited from 0.5 mm to 5 mm [50,61], while for mild to moderate rain rates, raindrop diameters range from 0.5 mm to 3 mm
- Raindrop density is assumed to be 1000 kg/m³
- **For a raindrop of 3mm diameter the mass is $m = 0.014$ gr**
- The maximum free falling terminal velocity levels out at around 9 m/s for diameters in excess of about 3.5 mm
- **Consider a terminal velocity of 8 m/s fully entrained in a horizontal 20 m/s wind** (i.e., assuming that the droplet is also travelling at this speed horizontally), strikes a **rotating blade with a 90 m/s tangential tip speed**, it is calculated that the **impact velocity between the rain and blade does not drop below 80 m/s**.
- Considering a time of contact through Impulse – Momentum theorem we conclude roughly to **a force of around 70 N !!!!!**



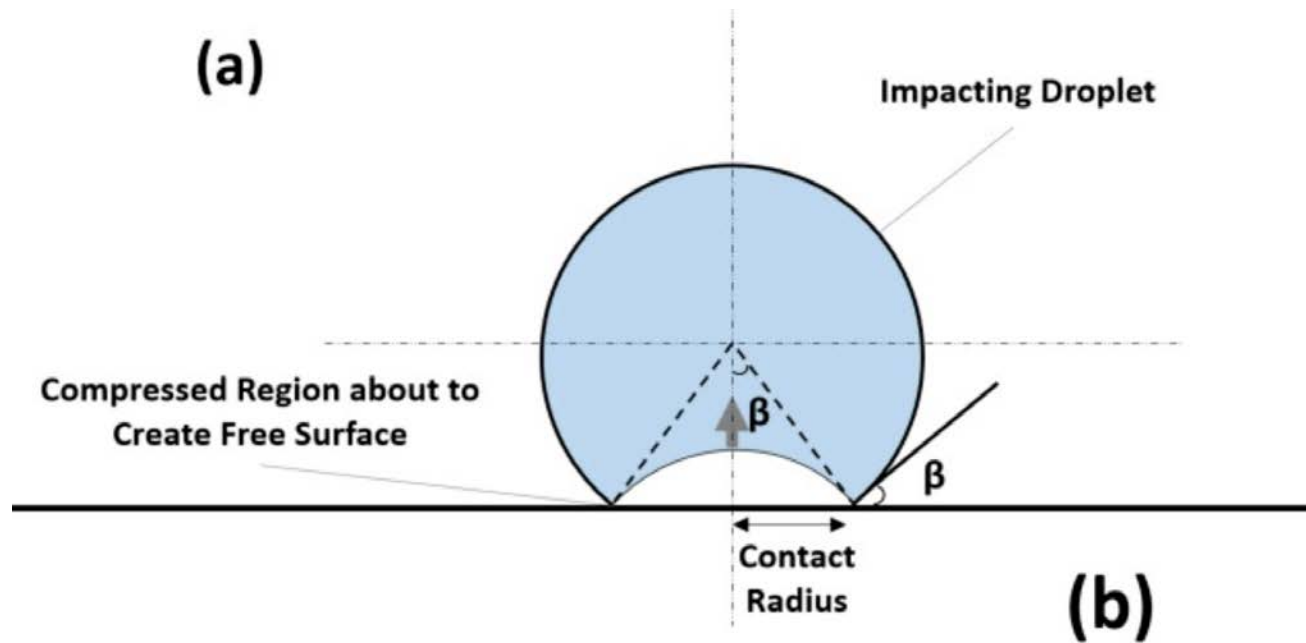
with spacial and temporal distribution ...

The physics behind the problem

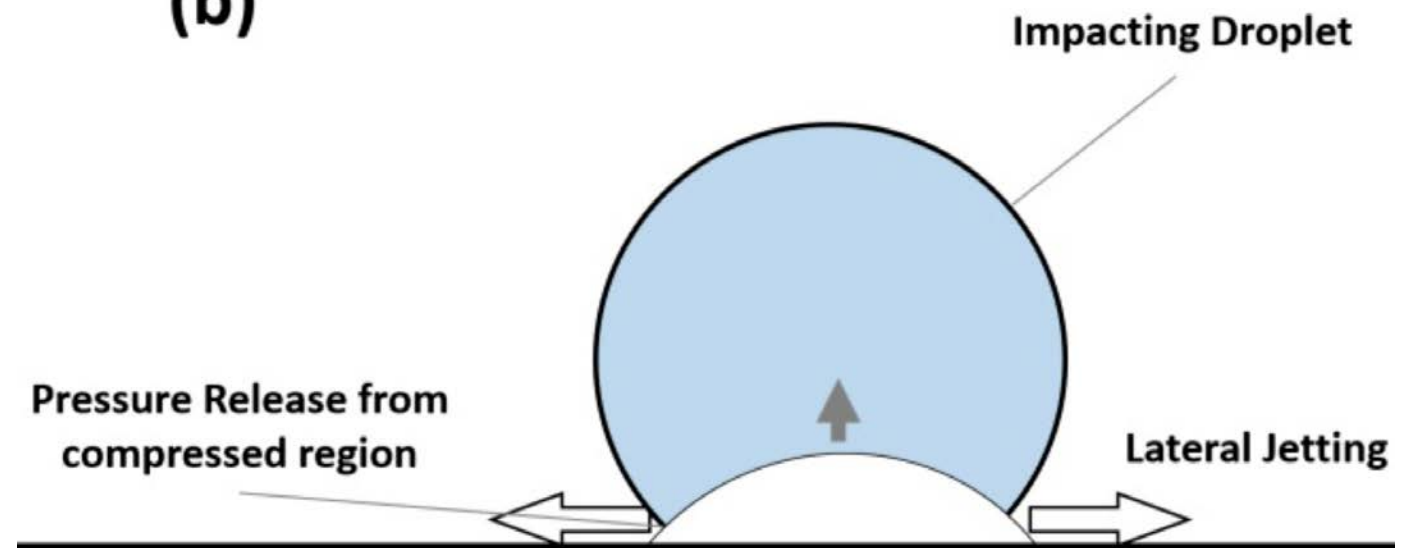


Three stress waves emerge from the impact zone to propagate this disturbance to the rest of the solid target, and therefore, shape its stress and strain field.

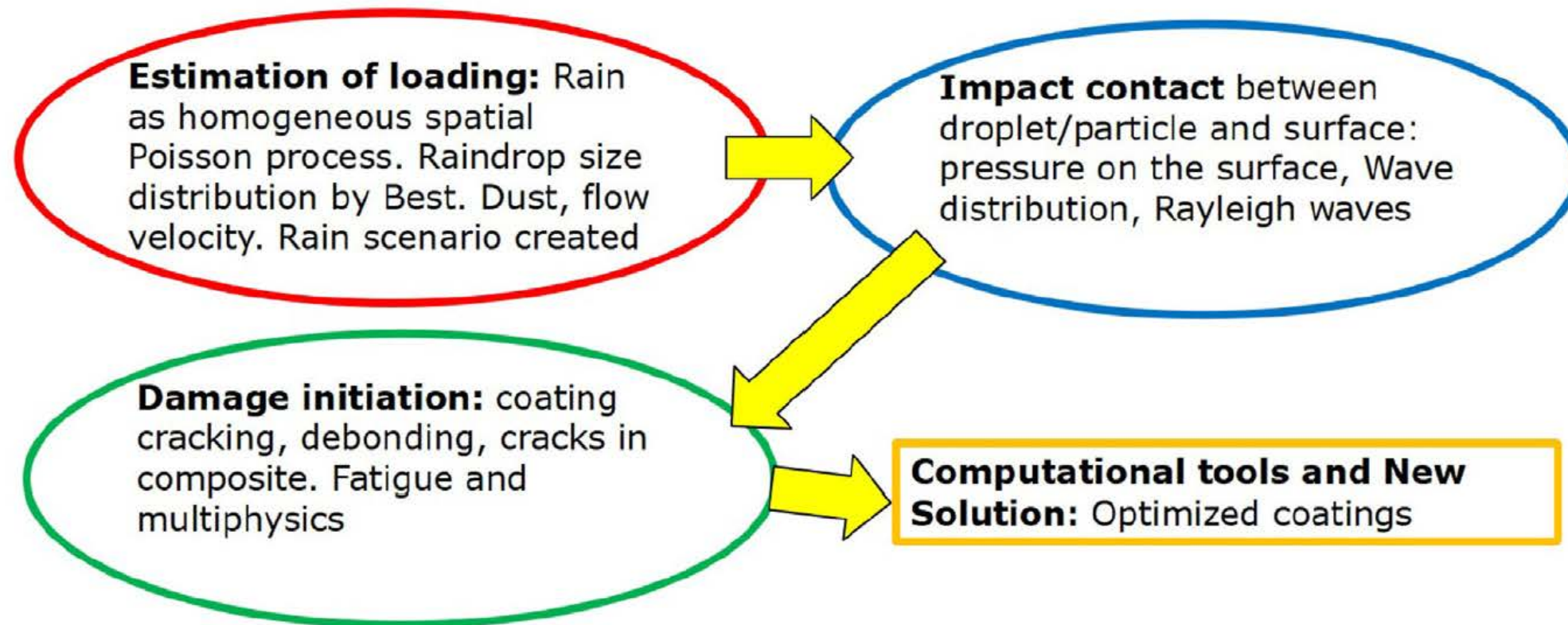
These waves are a **dilatational wave travelling in a longitudinal direction**, a **shear wave travelling in a transverse direction**, and a **Rayleigh wave moving along the surface**. Figure a illustrates the directions and the interaction of these stress waves.



As a first step of depressurizing the droplet, lateral outflow or jetting erupts from the contact zone shortly after impact moment. The jetting is expected to start when the shock front of the compressed liquid region propagating inside droplet creates a free surface



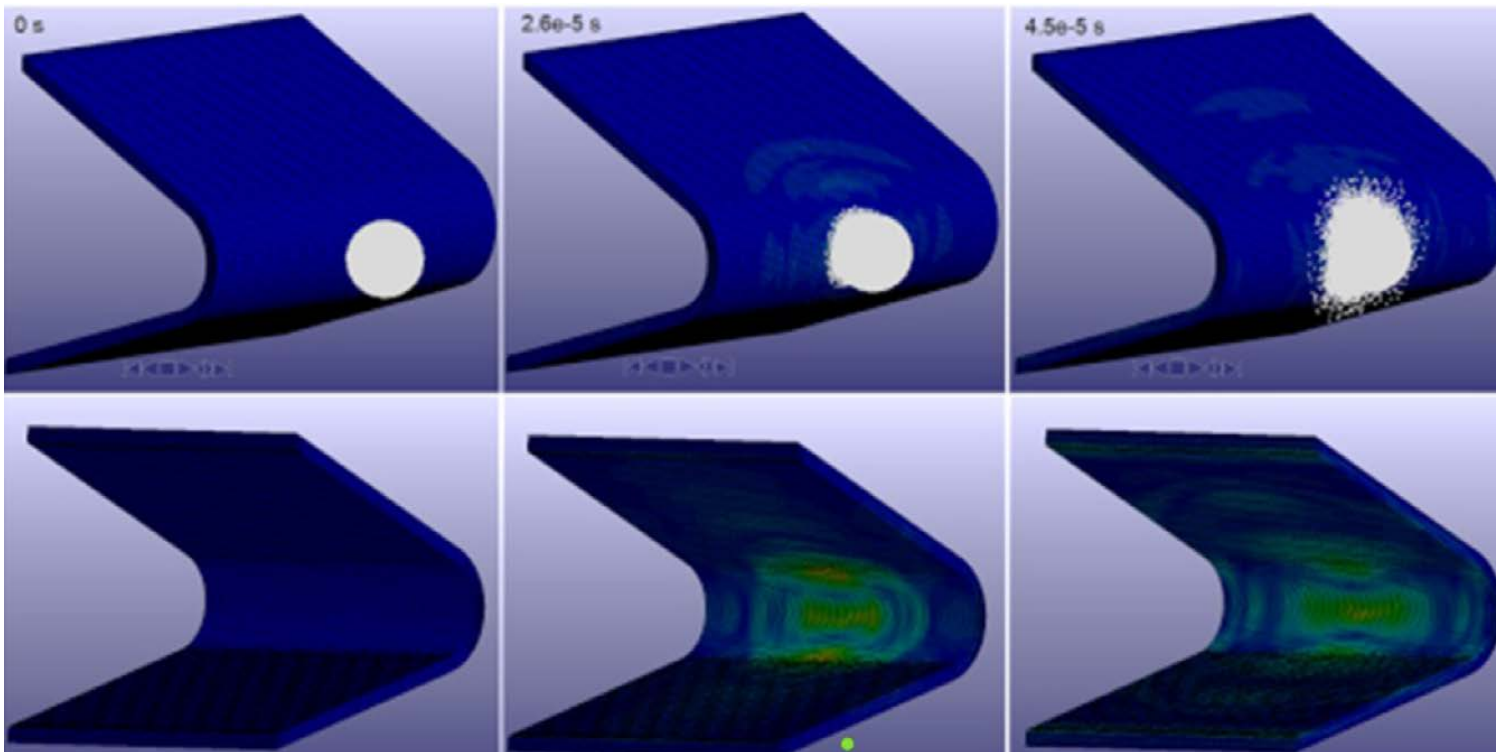
From a tribological point of view, and because of this high velocity, **the lateral jetting plays an important role in the initiation of the erosion damage as it can potentially tear surface irregularities.**



Schematic representation of the main steps of leading-edge erosion modelling

Hail Impact of Wind Turbine Blades

The scale of modern blades means that tip speeds in excess of 100m/s are now common in utility scale turbines. Coupling this with a hailstone terminal velocity ranging from 9m/s to 40m/s, the relative impact velocity becomes highly significant.

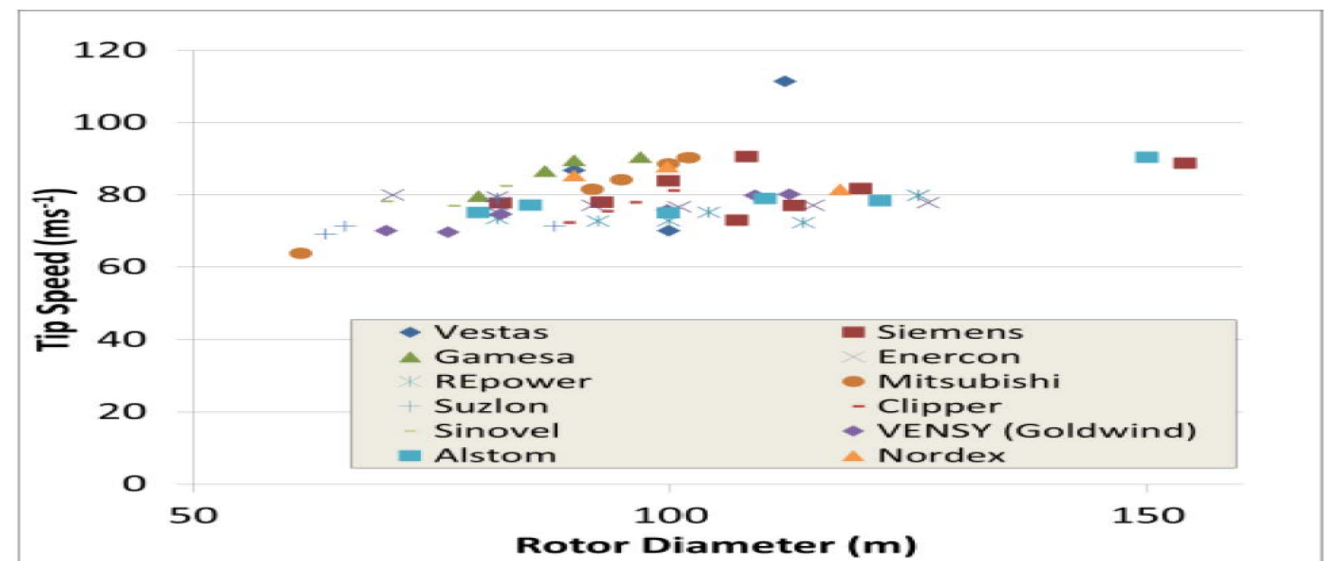


Hail Stone Impact on the Leading Edge

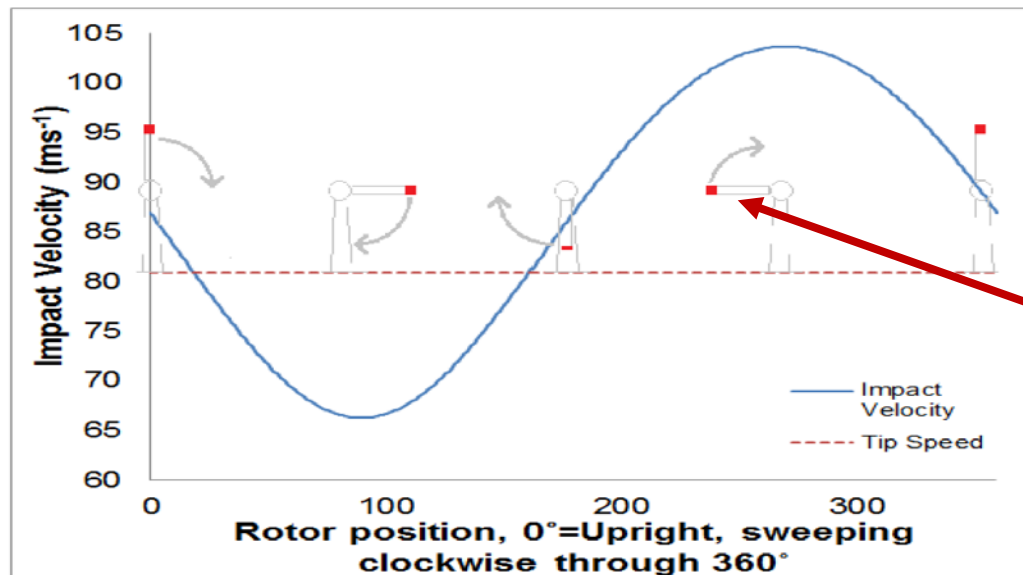
Hailstone Characteristics

- Hailstones can range in diameter from **5mm (the minimum size for hailstone classification)** to in excess of **50mm** in more extreme cases
- The terminal velocity of the hailstone is given by:

$$V_t = \sqrt{\frac{2m_h g}{C \rho_{air} A_h}}$$
 m_h is the mass of the hailstone, C is the drag coefficient of the hailstone, ρ_{air} is the air density and A_h is the cross sectional area of the hailstone.
- The frequency of hailstone impact events when compared to that of rain is much lower and will be heavily dependent on both site location and climatic conditions
- Wind Turbine Blade Tip Speed is given in the plot:



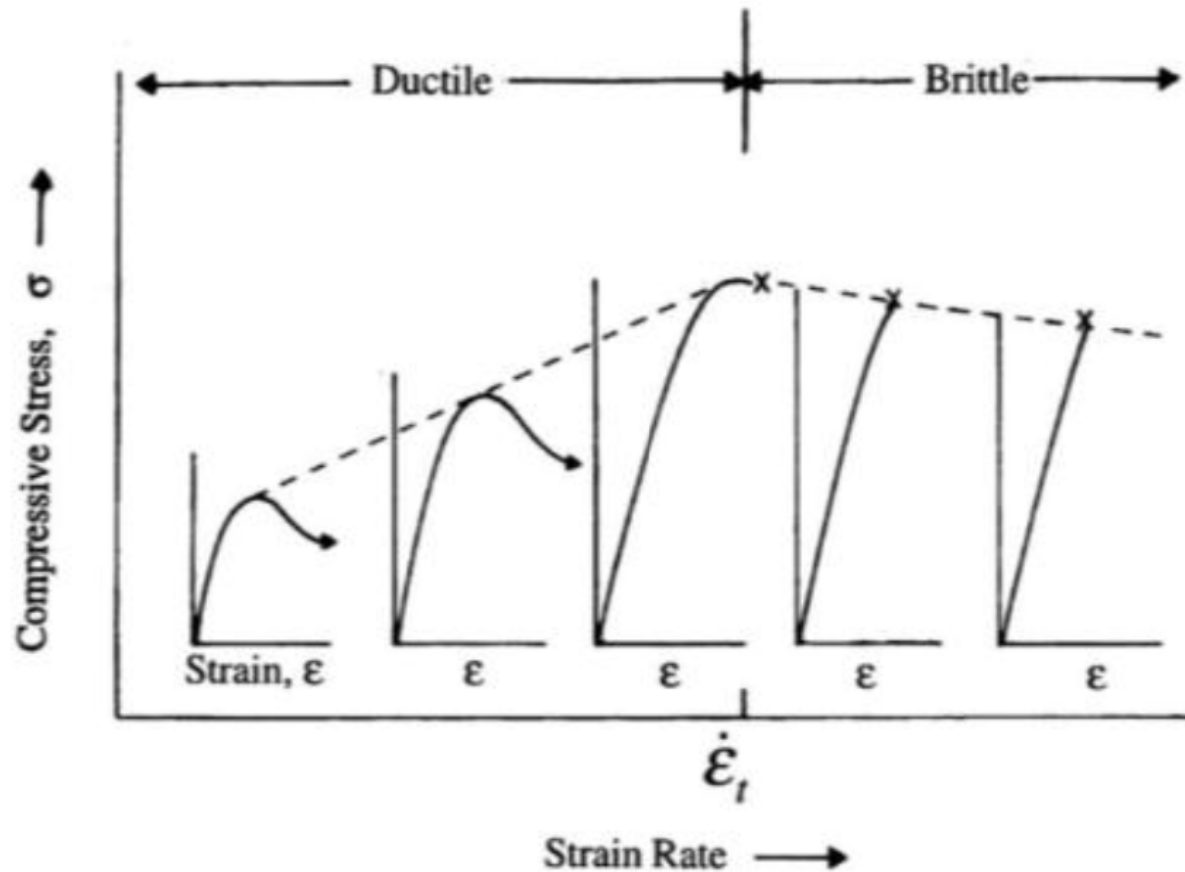
- The blade tip speed is only one influencing factor on the impact conditions at the leading edge of the blade. Two other important considerations are the terminal velocity of the hailstone and the incoming wind speed.
- Using the given data and doing a vectorial composition of the velocities, one may conclude to the hailstone impact velocity.
- For example, for a **20mm diameter hailstone with a density of 900kg/m³** falling at its theoretical terminal **velocity of 19.6m/s** striking the tip of a 45m long blade, rotating at 1.8 rad/s (81m/s tip speed), and assuming that the hailstone is fully entrained in a 25m/s wind (i.e. matches its horizontal velocity), the impact velocity can be calculated through a full rotor sweep, and it is given bellow:



at this rotor position the load on the blade (and therefore stress in the blade material) will also be high due to the cantilever/free hanging condition!!!

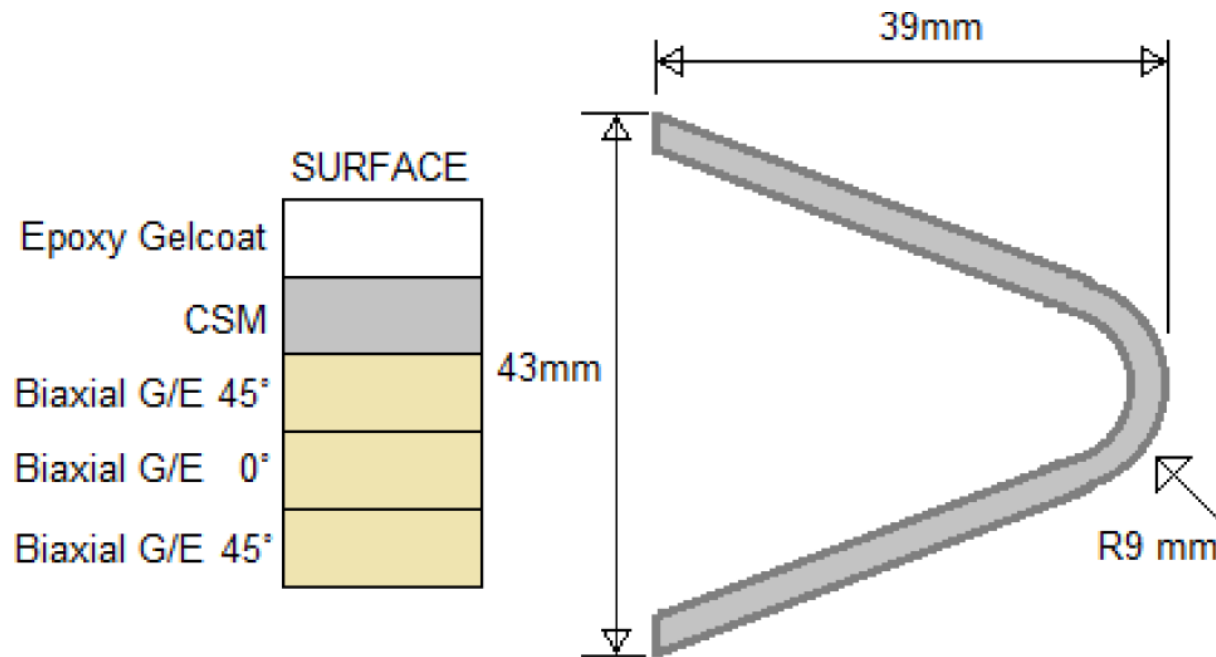
Materials

- blade designs feature composites made from a thermosetting plastic (commonly epoxy or polyester) with either glass or carbon fiber reinforcement. They are delamination prone.
- Gelcoats can be applied in-mould if they are similar to the matrix material employed in the structural composites (epoxy, polyester etc.) or applied through spraying/painting once the blade is removed from the mould.
- Leading edge protection tape can also be applied, typically at sites where leading edge erosion is an issue
- Unlike Gelcoats which are typically made of tough and stiff resins such as epoxy or polyester, leading edge tapes are typically made of polyurethanes which are more ductile and absorb impact energy through deformation.
- Ice is a complex and highly variable material with regards to its material characteristics and properties and as such is widely considered as a class of material rather a single type. Ordinary ice is said to possess a density of 917kg/m³ and this value increases somewhat with a decrease in temperature.
- The ice has strain dependent characteristics and the transition from ductile to brittle behavior is reported to occur at a strain rate of the order of 10⁻³ (1/s).



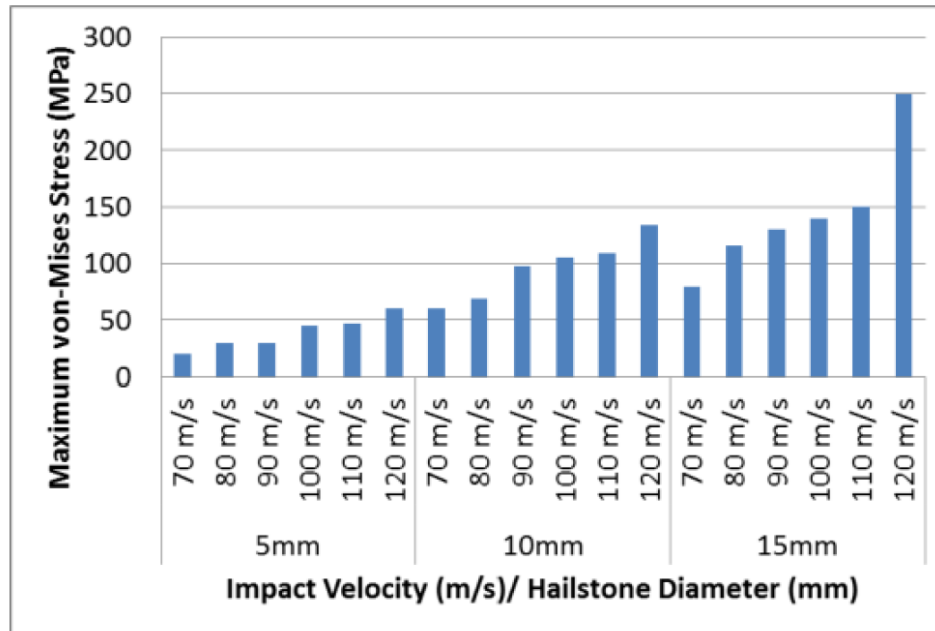
Compressive behaviour of ice,

For the modeling of the strain rate dependent behavior of the hailstone Eulerian or Smooth Particle Hydrodynamics approach will be used. The results obtained for both the Eulerian and SPH approaches compared very closely both quantitatively and qualitatively. However, the computational time required for the SPH approach was significantly less.

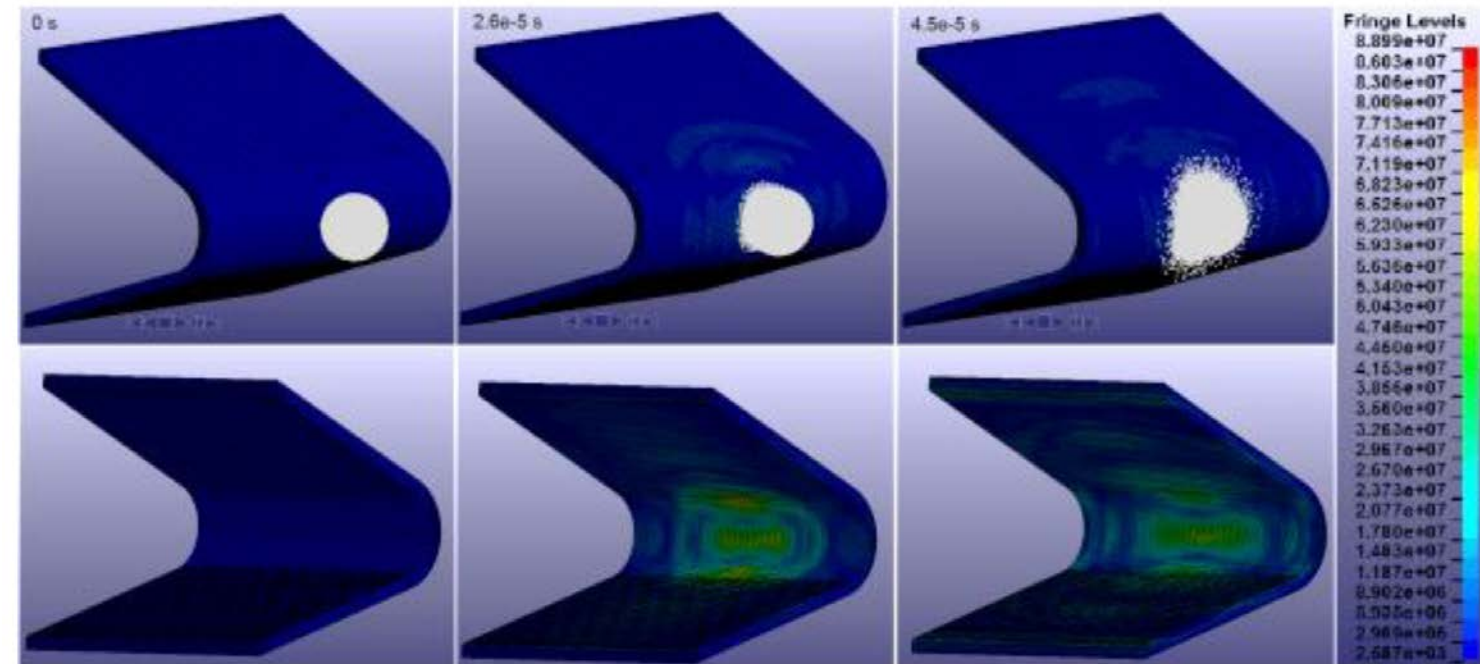


Material	Epoxy Gelcoat	CSM
Source	Various	Various
Density	1400	1100
Young's Modulus (GPa)	7	3.5
Poissons Ratio	0.33	0.33
Tensile Strength (MPa)	80	65
Elongation at break (%)	1.6	3
LS-DYNA Material Model	MAT_003	MAT_003

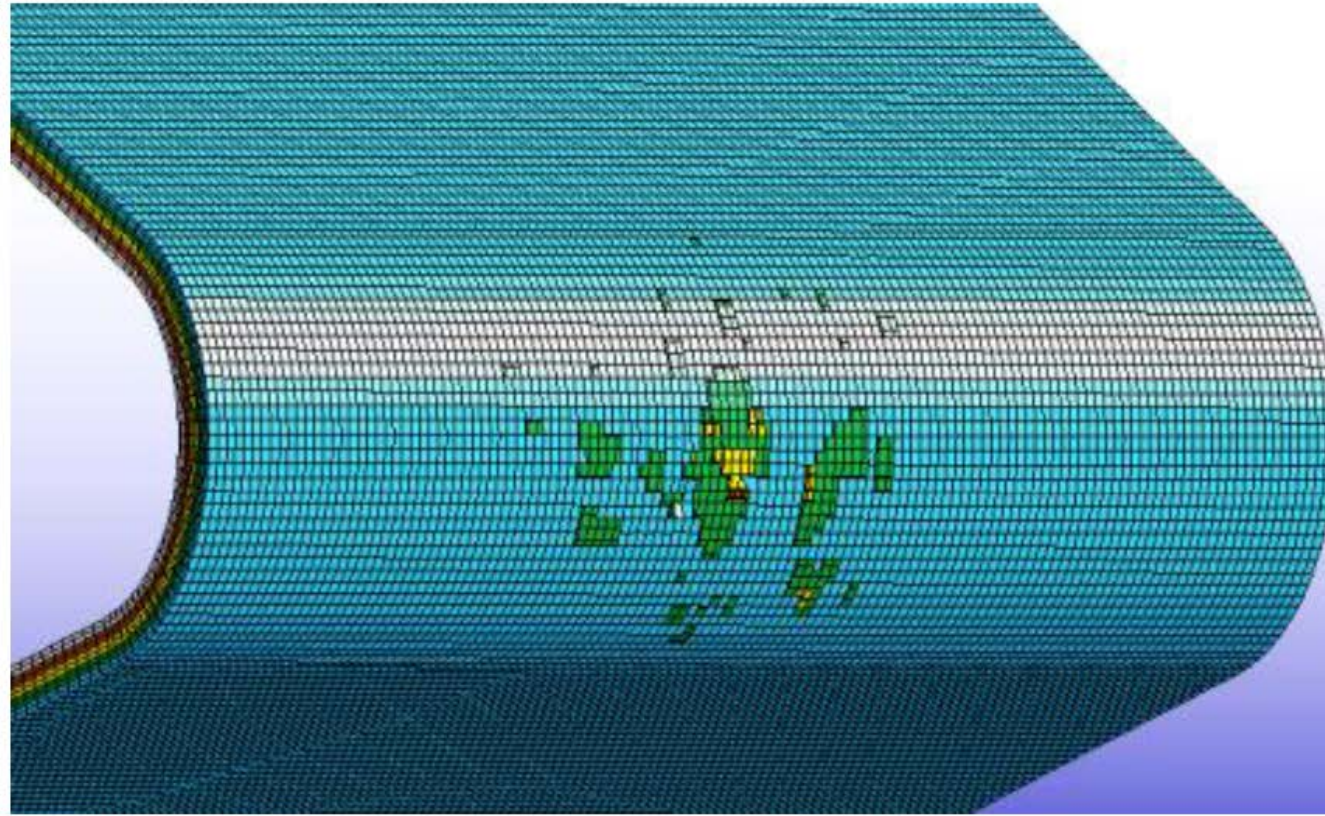
Orientation	Young's Modulus (GPa)	Tensile Strength (MPa)	Compressive Strength (MPa)
1	26	414	458
2	26	414	458
3	8	120	500
	Shear Modulus (GPa)	Shear Strength (MPa)	Poissons Ratio
12	3.8	105	0.1
23	2.8	65	0.25
13	2.8	65	0.25
	Interlaminar Normal Failure Stress (MPa)	Interlaminar Shear Failure Stress (MPa)	Strain Failure (%)
	35	65	1.81



Maximum impact stress across hailstone diameters and velocities



10mm diameter hailstone impact at 100ms^{-1} . contours of von-Mises Stress

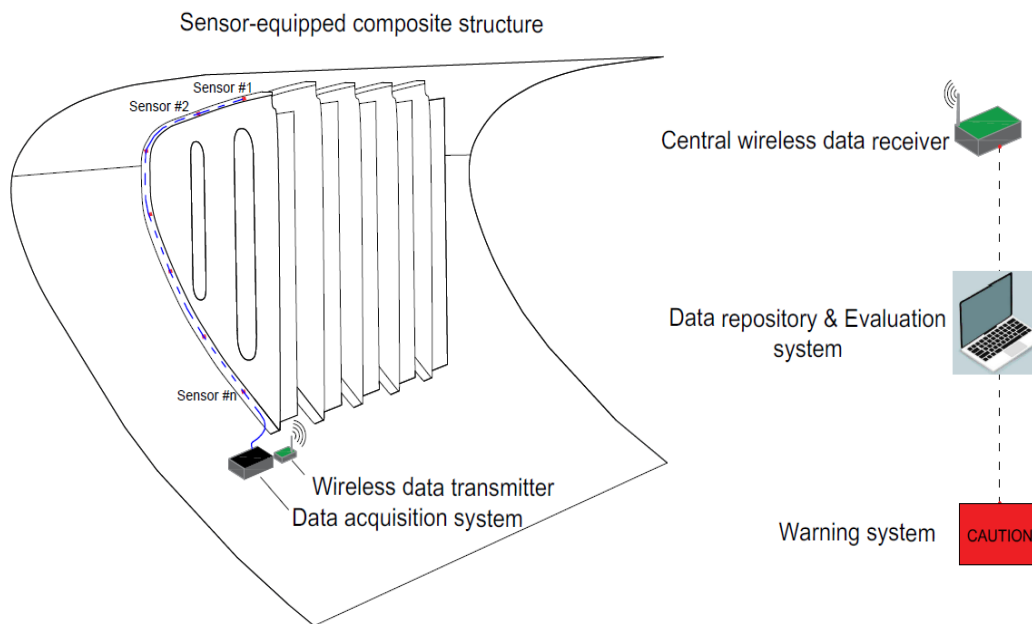


Results from erosion prediction,
15mm diameter hailstone at 100ms^{-1} impact

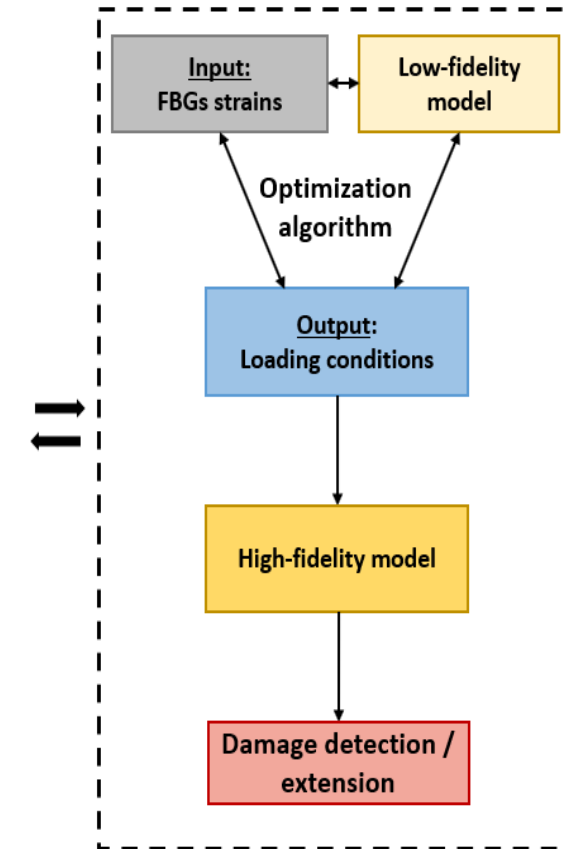
How to calculate damage due to hailstone impact events (a recent approach)

CONCEPT

- Digital twin-based algorithm for the damage localization and quantification (named Damage Evaluation Algorithm-DEA)
- Principle of operation based on strain histories comparisons
- LF and HF physical-based model are employed

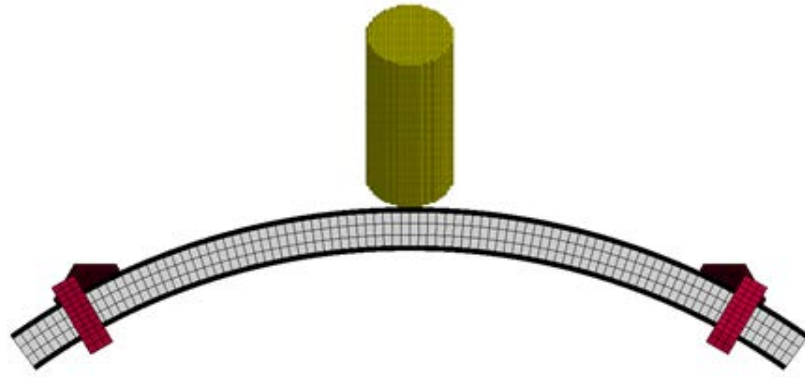


Schematic of digital-twin-based damage diagnosis concept, Source: E. Giannaros

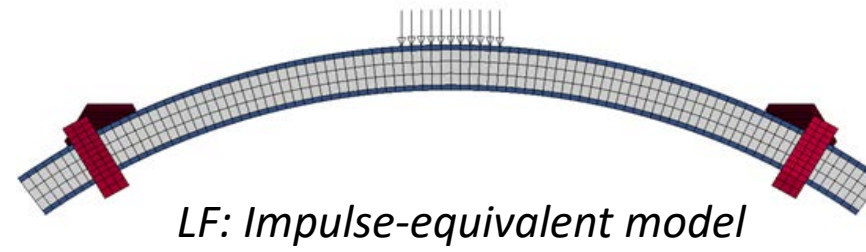


Low- and High-fidelity modeling & validation

- Physical-based FE models with different fidelity

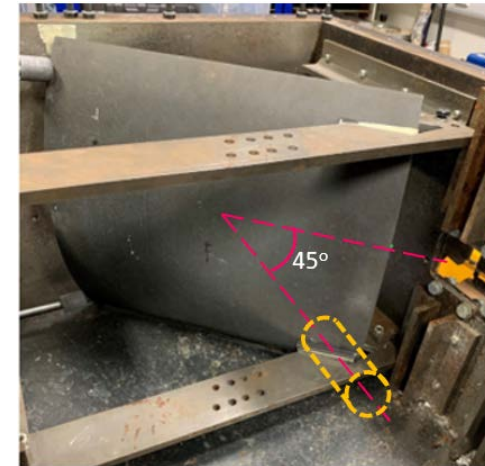
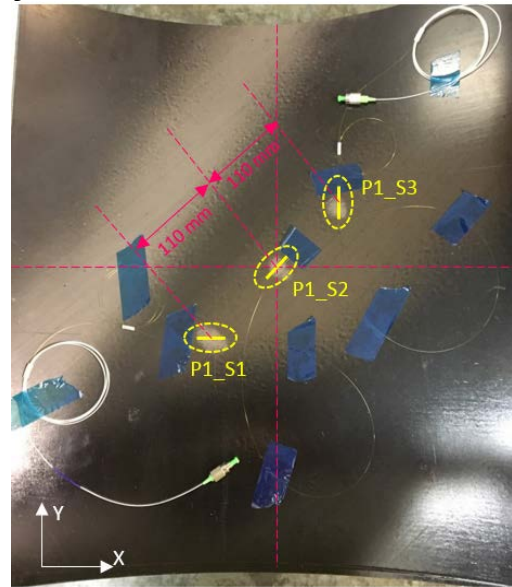


HF: Model including SPH soft projectile



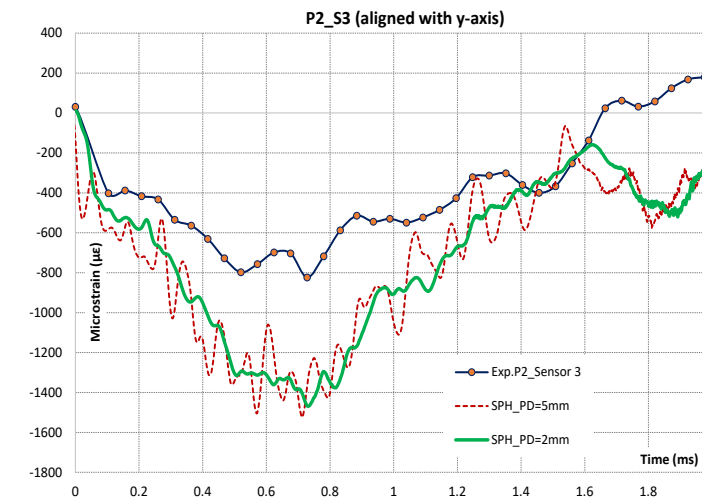
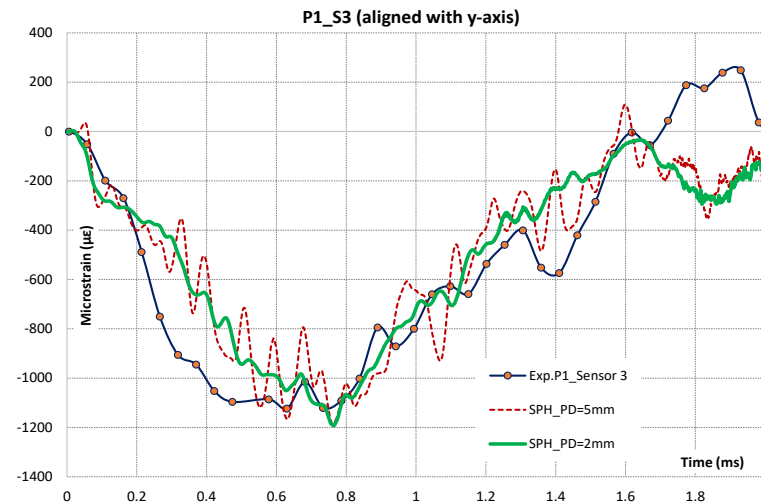
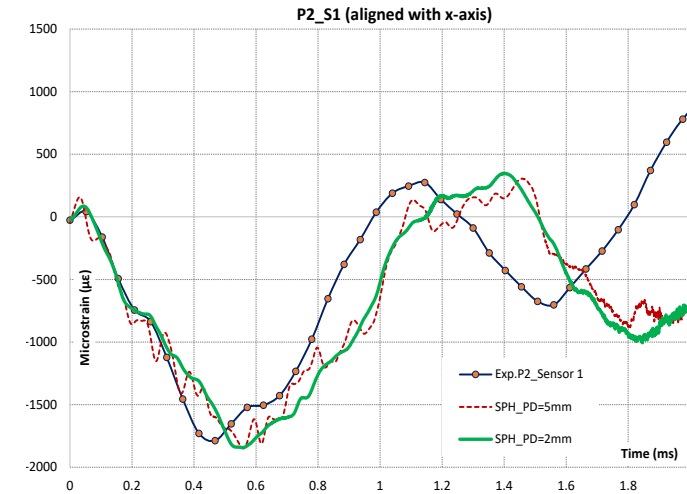
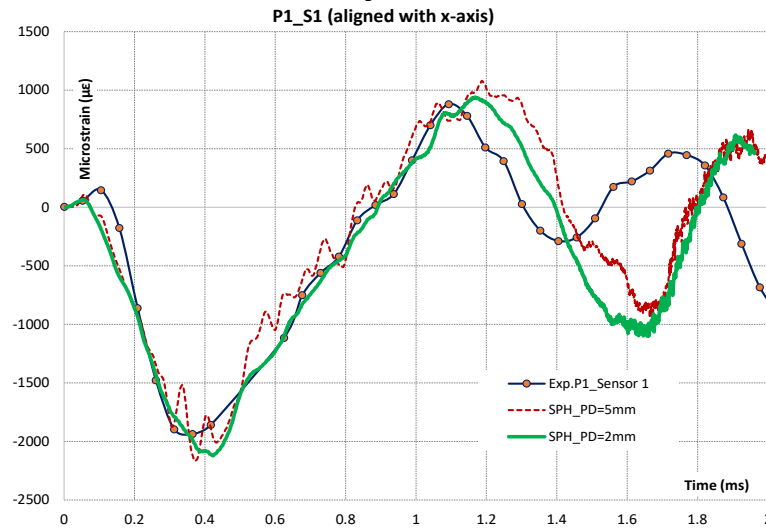
LF: Impulse-equivalent model

*Soft body impact tests
(UBRUNEL)
& FBGs placement*



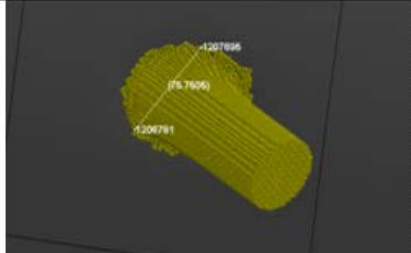
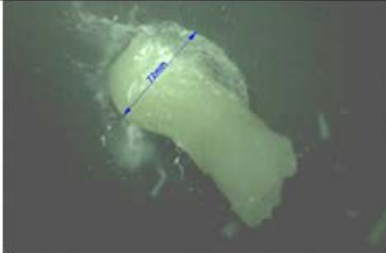
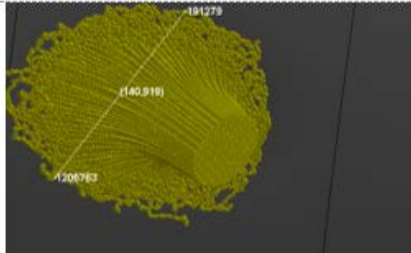
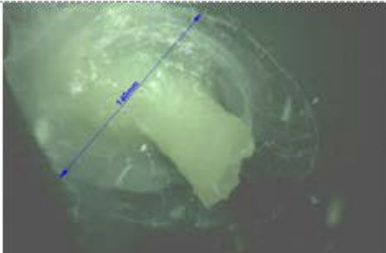
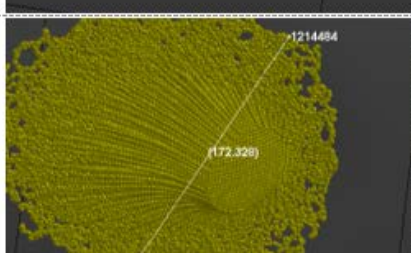
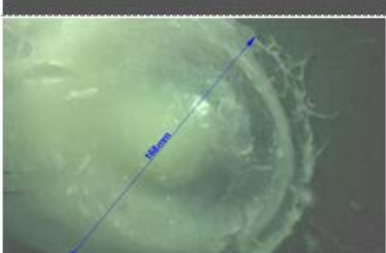
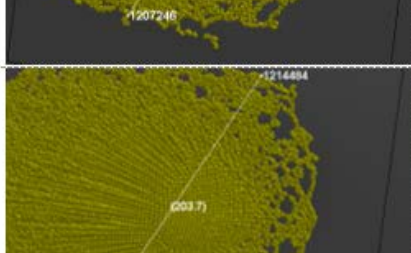
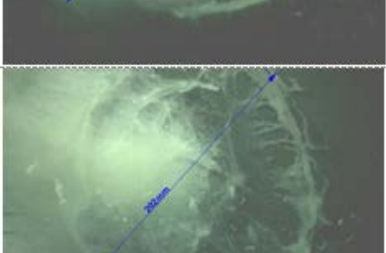
Low- and High-fidelity modeling

HF mode results vs. Experiments (Strain histories: 5 evaluations criteria)

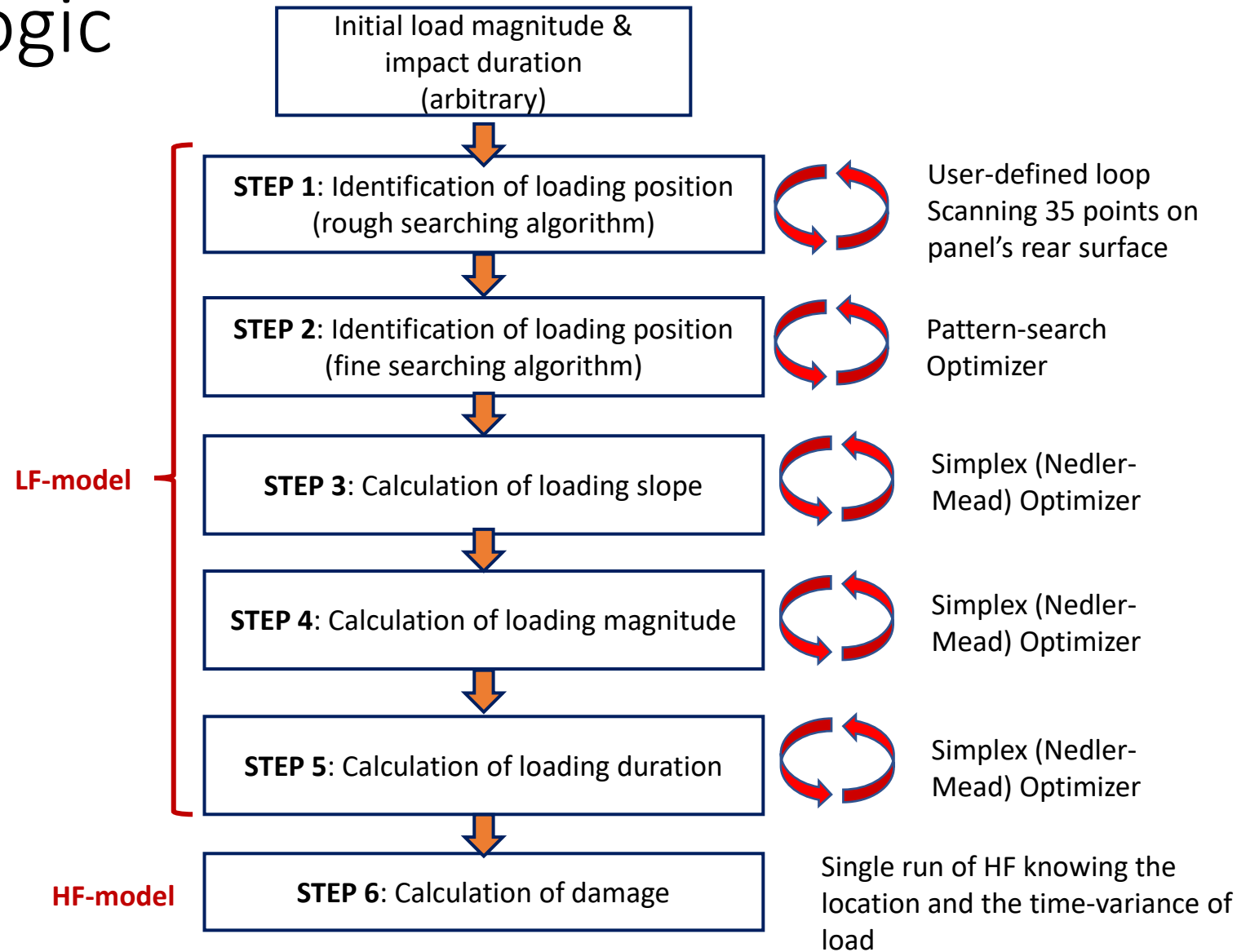


Low- and High-fidelity modeling

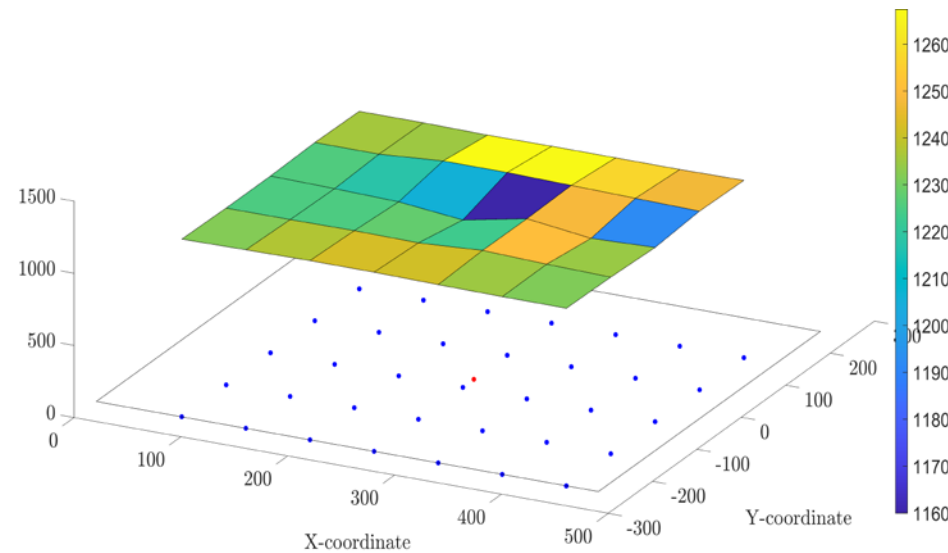
Evolution of soft body deformation

Time	HF model-2mm PD	Test	Comparison
0.50 ms			Num: 76 mm Exp: 72 mm
0.70 ms			Num: 141 mm Exp: 140 mm
0.90 ms			Num: 172 mm Exp: 168 mm
1.10 ms			Num: 204 mm Exp: 202 mm

Algorithm logic

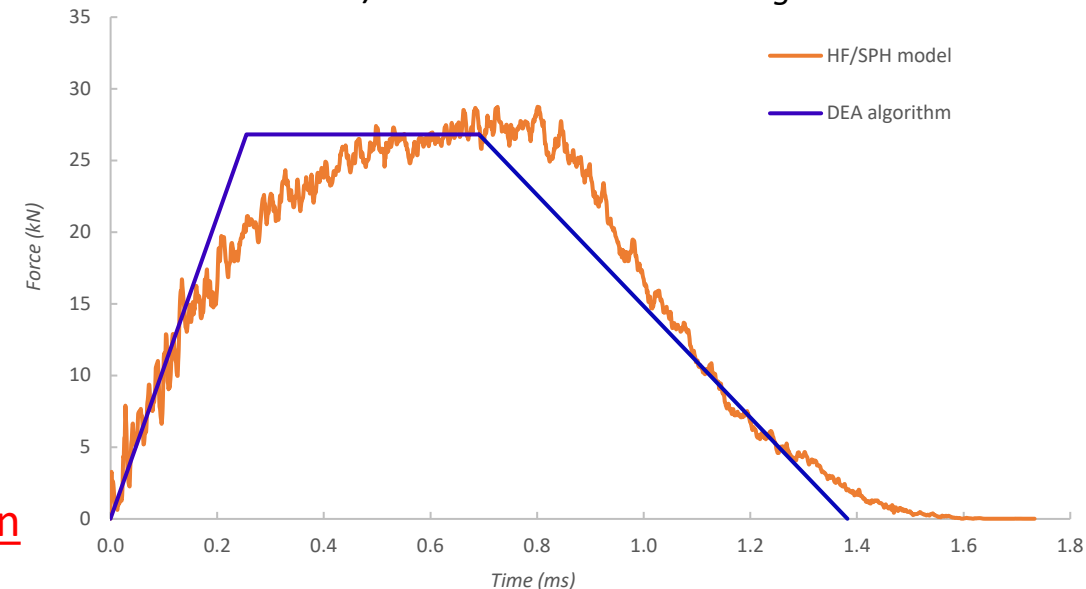


DEA algorithm's effectiveness



RMSE between numerical and target strain-time histories for 1st step of algorithm

Contact force-time response derived from LF/SPH model and the DEA algorithm



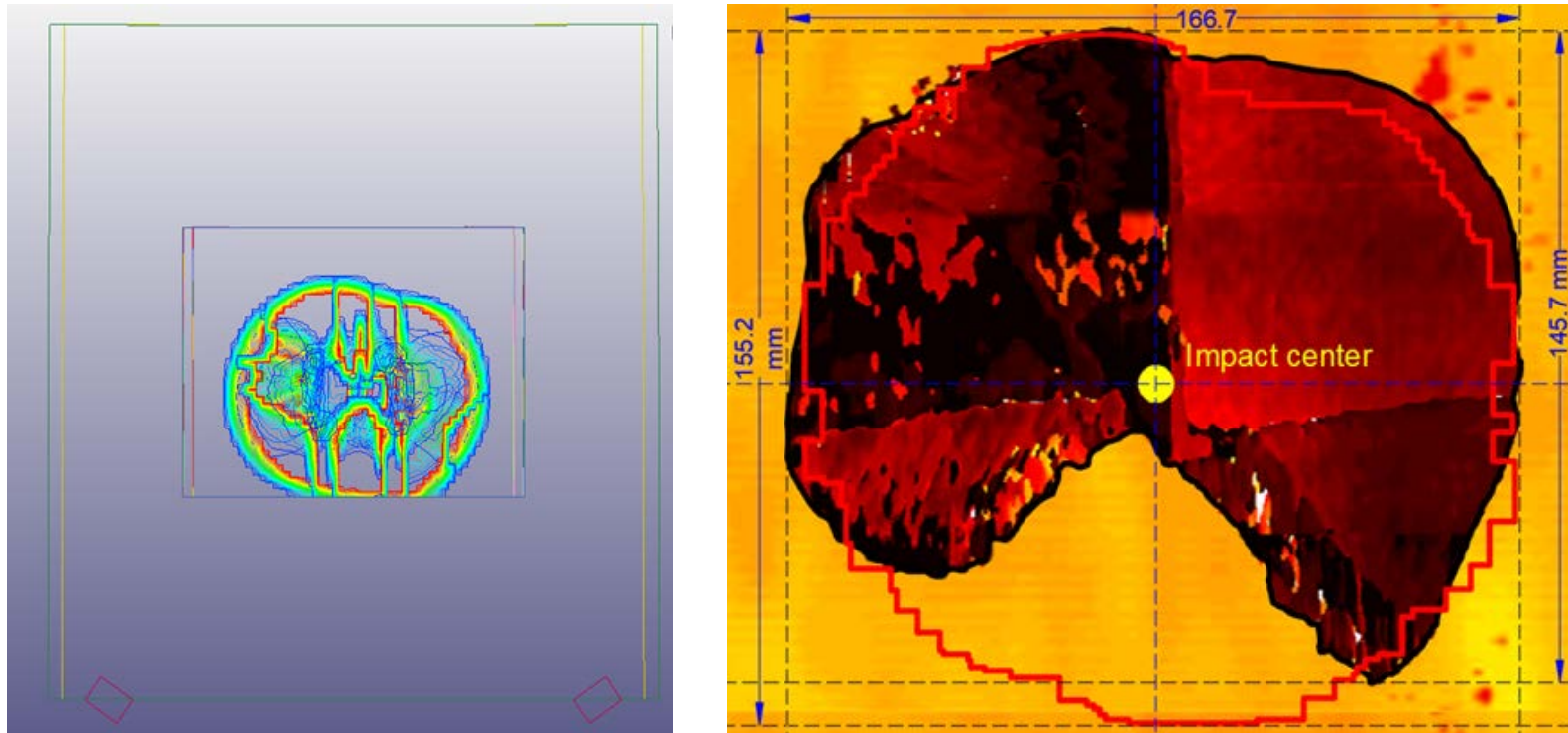
HF-SPH model : 24.6 Ns

DEA code : 24.3 Ns

✓ 1.2 % error to impulse calculation

Interlaminar damage comparison

Comparison of total numerical delamination damage (red line) with the experimental one (black line) (right) and model with numerical delamination damage (left).



Non-destructive evaluation (Prof.M.Meo, UBATH)

- ✓ The location and the extent of the actual damage in both directions have been precisely captured from the DEA algorithm

Snow effect on the blades

Atmospheric icing is defined as the accretion of ice or snow on structures exposed to the atmosphere. Two different types of atmospheric icing can be distinguished: in-cloud icing (**rime ice** or glaze) and precipitation icing (**freezing rain** or drizzle, **wet snow**).

Rime ice is formed when the wind transfers supercooled liquid water droplets from clouds or fog. These droplets might freeze instantaneously as they hit a surface. In the case of small droplets, soft rime is formed, while hard rime is formed by large droplets.

Soft rime usually ranges in density from 200 kg/m³ to 600 kg/m³

Hard rime ice density ranges typically between 600 kg/m³ and 900 kg/m³

The formation of rime ice is asymmetrical, usually taking the shape of needles following the windward side of a structure. Rime ice is typically formed at temperatures from -20 °C to 0 °C.

Glaze/Freezing Rain: Glaze is the result of freezing rain or wet in-cloud icing. A smooth, transparent and homogenous ice layer is formed and strongly adheres on surfaces. Glaze is usually formed at temperatures from 0 °C to -6 °C with a density of around 900 kg/m³. Freezing rain occurs when the air aloft does not let water at temperatures below freezing to form ice crystals.

Wet snow is formed by partially melted snow crystals with high liquid water content. The liquid content of the crystals increases the cohesive forces of this formation. Thus, it is able to adhere on an object's surface. Wet snow accretion occurs when the air temperature is between 0 °C and +3 °C, with typical density from 300 kg/m³ to 600 kg/m³.

Apart from the aforementioned categorisation, the icing conditions at a site are further described by the following additional parameters:

- **icing rate: ice accumulation per time (kg/h)**
- **maximum ice load: maximum ice mass accreted at a structure (kg/m)**



Effects of blades icing

Ice accretion on the wind turbine blades produces significant change in the geometry of each blade's surface, affecting its aerodynamic efficiency. As a result, the blade lift reduces while the drag increases, resulting in reduced power production and, eventually, in the turbine's shutdown. Reduced power production occurs with an increasing number of lower than expected power stops, stops due to high vibration amplitude and stops due to faulty wind measurements.

Apart from the reduction in produced electricity, **increasing vibrations and aerodynamic noise, imbalances in the blades, leading to increased wear in structural components such as connectors, couplers and gearbox, errors in nacelle wind speed measurements**, as well as the risk of ice throw resulting in safety hazards

Asymmetrical icing of the blades **induces loads and vibrations in the tower, hub and nacelle assembly at a frequency synchronous to rotational speed of the turbine, imposing considerable fatigue loads. The aerodynamic changes in the iced blade can cause violent vibrations within the wind velocity operating range of the Turbine.**